



D E2.7 – FWA over long optical links

Gert-Jan Rijckenberg
Anthony Ng'oma
Kun Wang
Eva Rojas Alonso
Ton Koonen

Den Dolech 2
P.O. Box 513
5600 MB Eindhoven
The Netherlands
e.m.rojas.alonso@tue.nl
a.m.j.koonen@tue.nl

Identifier:	Deliverable D E2.7
Class:	Report
Version:	6
Version Date:	31/03/2008
Distribution:	Public
Responsible Partners:	TUe
Filename:	DE2-7_v06.doc

DOCUMENT INFORMATION

<i>Project ref. No.</i>	IST-6thFP-026442
<i>Project acronym</i>	MUSE II
<i>Project full title</i>	Multi-Service Access Everywhere
<i>Security (distribution level)</i>	Public
<i>Contractual delivery date</i>	M51
<i>Actual delivery date</i>	31/03/2008
<i>Deliverable number</i>	D E2.7
<i>Deliverable name</i>	FWA over long optical links
<i>Type</i>	Report
<i>Status & version</i>	Final, version 6
<i>Number of pages</i>	48
<i>WP / TF contributing</i>	WPE2
<i>WP / TF responsible</i>	WPE2
<i>Main contributors</i>	TUE
<i>Editor(s)</i>	G-J Rijckenberg, A Ng'oma, K Wang, E Rojas Alonso
<i>EU Project Officer</i>	Pertti Jauhiainen
<i>Keywords</i>	
<i>Abstract (for dissemination)</i>	This document describes tests and evaluations of a Radio over Fibre system for the use of Fixed Wireless Access over long optical links. The document outlines the importance of the dispersion tolerance of the employed system.

DOCUMENT HISTORY

Version	Date	Comments and actions	Status
1	31-05-07	TOC	First draft
2	18-06-07	new TOC	First draft
3	6-8-07	changes	First draft
4	8-8-07	Integration of all contributions	Second draft
5	30-8-07	Comments from reviewers	Final draft
6	31-03-08	Update of additional information	Final

EXECUTIVE SUMMARY

In the framework of the XL-PON node consolidation activities in the IST project MUSE, alternative ways to achieve node consolidation are developed. One of these alternatives is Fixed Wireless Access (FWA) based on Radio over Fibre (RoF). A major property of a RoF system is that radio access points or base stations are significantly simplified through the consolidation of signal processing functions in the headend. In addition wireless access has the inherent advantage of being able to reach all users and FWA can be deployed in areas or buildings where it is difficult or impossible to deploy wired infrastructure (xDSL (Digital Subscriber Line) / fibre).

MUSE investigated a cost-effective and WiMAX compliant solution to implement RoF to feed base stations for FWA in Phase I as an alternative to the conventional digital baseband feeders deployed today. Although the co-existence of this RoF system with the XL-PON (eXtra Large Passive Optical Network) developed in MUSE is an interesting research topic, it was decided to focus on its ability to transport FWA services over long optical links. A challenge in the new XL PON is to achieve a RoF system that operates over fibre lengths up to 100 km and thus has to face disturbances like chromatic dispersion and other non-linearities.

This document presents results on the non-linear characteristics of the RoF system, including experimental findings and theoretical work. The Optical Frequency Multiplication (OFM) system is employed for FWA. OFM involves the interferometric filtering of a frequency modulated optical signal and the resulting FM-IM (frequency modulation – intensity modulation) conversion is used to optically up-convert carrier frequencies.

OFM can be used to combat chromatic dispersion-induced fading, enabling flexible extra-long RoF links for distributing pure high-frequency signals. In laboratory experiments, a high quality 22.2 GHz signal was transmitted over various fiber lengths up-to 72 km without any fading. The measured OFM link length was at least 15 times longer than that of the corresponding IM-DD (intensity modulation – direct detection) system. The transmission of a high quality 100Mbps, 16 QAM signal at the frequency of 39.9 GHz over a 50 Km fibre length without any fading has also been demonstrated.

A model has been developed, which describes the behaviour of the OFM system in the presence of chromatic dispersion. Model simulations showed that no fading occurs in the system. Laboratory experiments confirmed this predicted behaviour. It is further observed that both the interferometric filtering and the fibre chromatic dispersion contribute to the generation of RF carriers. The best performance of the OFM system against chromatic dispersion was found to occur when the system was optimized for maximum harmonic power generation (e.g. by appropriate filter biasing) prior to fibre transmission.

The impact of SBS (Stimulated Brillouin Scattering) on both the links lengths and the signal quality transmission of both IM-DD and OFM RoF systems was studied experimentally and compared. It was observed that the OFM system exhibited a much lower SBS threshold (6 dB) than the IM-DD system. The performance of the OFM system in terms of the quality of the transmitted signal was also found to be much better than that of the IM-DD system. Measurement results showed that longer RoF link lengths are feasible when the OFM technique is used. SBS measurement results also showed that the signal frequency has no impact on the SBS threshold and the performance of the IM-DD system.

As optical amplifiers will be needed in an XL PON architecture to cover the fibre and splitter losses, the impact of ASE (Amplified Spontaneous Emission) on the RoF quality needs to be evaluated. Laboratory measurements show the effects of ASE noise do not affect the transmission and the system performance in the OFM system.

TABLE OF CONTENTS

DOCUMENT INFORMATION	2
DOCUMENT HISTORY	3
EXECUTIVE SUMMARY	4
TABLE OF CONTENTS	6
LIST OF FIGURES AND TABLES	7
ABBREVIATIONS	9
1 INTRODUCTION	13
2 APPROACH	15
2.1 Overview	15
2.2 IM-DD Dispersion model	15
2.3 OFM Dispersion model	16
2.4 Experimental approach	19
3 THEORETICAL RESULTS	20
3.1 OFM dispersion model analysis	20
3.1.1 Sensitivity analysis	20
3.1.2 OFM chromatic dispersion tolerance	22
3.2 Discussion	25
4 EXPERIMENTAL RESULTS	27
4.1 Experiments	27
4.1.1 Dispersion impact assessment	27
4.1.2 OFM link loss budget	30
4.1.3 Impact of EDFA noise	33
4.1.4 Impact of non-linearities	35
4.2 Dispersion tolerance and model validation	44
5 CONCLUSIONS AND DISCUSSION	46
REFERENCES	48

LIST OF FIGURES AND TABLES

FIGURE 1-1 THE XL PON WITH INTERCONNECTED FWA FEEDER SYSTEM	13
FIGURE 2-1 BASIC SCHEME FOR THE OFM MODEL	15
FIGURE 3-1 OFM DISPERSION BEHAVIOUR (5 TH HARMONIC)	21
FIGURE 3-2 IM-DD DISPERSION BEHAVIOUR.....	22
FIGURE 3-3 OFM FREQUENCY SPECTRUM (WITH THE EVEN HARMONICS SUPPRESSED) IN B2B CONFIGURATION	23
FIGURE 3-4 OFM FREQUENCY SPECTRUM (WITH THE EVEN HARMONICS SUPPRESSED) AFTER 25 KM OF SMF	23
FIGURE 3-5 INFLUENCE OF MZI FILTER BIASING ON THE BEHAVIOR OF THE OFM SYSTEM.....	24
FIGURE 3-6 SIMULATED INTERACTION COMPONENTS OF 5 TH HARMONIC, F_M IS 4.4 GHZ FOR DIFFERENT FIBRE LENGTHS	25
FIGURE 4-1 LABORATORY SET-UP FOR MEASURING THE IMPACT OF CHROMATIC DISPERSION ON THE IM-DD AND THE OFM ROF SYSTEMS.....	27
FIGURE 4-2 MEASURED IMPACT OF CHROMATIC DISPERSION ON IM-DD AND OFM ROF SYSTEMS, INCLUDING THE THEORETICAL PREDICTION FOR OFM.....	28
FIGURE 4-3 SPECTRUM OF AN OFM UP-CONVERTED SUB-CARRIER AND CONSTELLATION DIAGRAM OF THE 100 MBPS 16-QAM @ 22.4 GHZ DATA RECOVERED AFTER TRANSMISSION ON 50 KM SMF.....	29
FIGURE 4-4 SPECTRUM OF AN OFM UP-CONVERTED SUB-CARRIER OF THE 100 MBPS 16-QAM @ 39.9 GHZ DATA RECOVERED AFTER TRANSMISSION ON 50 KM SMF	30
FIGURE 4-5 CONSTELLATION DIAGRAM OF THE 100 MBPS 16-QAM @ 39.9 GHZ DATA RECOVERED AFTER TRANSMISSION ON 50 KM SMF	30
FIGURE 4-6: MEASUREMENT SET-UP FOR THE OFM LINK LOSS BUDGET.....	30
FIGURE 4-7 EXPERIMENT SET-UP FOR EDFA ASE NOISE ASSESSMENT.....	33
FIGURE 4-8 OPTICAL SPECTRUMS COMPARISON WITH EDFA INPUT POWER AT -19.5 DBM.....	34
FIGURE 4-9 OPTICAL SPECTRUMS COMPARISON WITH EDFA INPUT POWER AT -10.5 DBM.....	34
FIGURE 4-10 MEASUREMENT SET-UP FOR THE IMPACT OF MODULATION DEPTH ON THE SBS THRESHOLD.....	36
FIGURE 4-11: MEASURED IMPACT OF PHASE MODULATION DEPTH ON THE SBS THRESHOLD VALUE FOR SWEEP POWER EQUALS (A) -30 DBM, (B) -12 DBM, (C) -8 DBM, AND (D) COMPARISON.....	36
FIGURE 4-12 IMPACT OF FIBRE LENGTH ON SBS THRESHOLD	37
FIGURE 4-13 LABORATORY SET-UP FOR COMPARING THE PERFORMANCES OF THE IM-DD AND THE OFM ROF SYSTEMS AGAINST SBS	38
FIGURE 4-14 MEASURED IMPACT OF SBS ON SIGNAL QUALITY TRANSMISSION IN AN IM-DD ROF SYSTEM FOR THE FREQUENCIES (A) 200 MHZ, (B) 2.2 GHZ, (C) 18 GHZ, AND (D) COMPARISON.....	39
FIGURE 4-15 IMPACT OF SIGNAL FREQUENCY ON THE PERFORMANCE OF THE IM-DD SYSTEM AGAINST SBS	40
FIGURE 4-16 COMPARISON OF THE PERFORMANCES OF THE IM-DD (18 GHZ) AND THE OFM (22 GHZ) ROF SYSTEMS AGAINST SBS (A) 25 KM SMF, (B) 50 KM SMF.....	41
FIGURE 4-17 PERFORMANCE COMPARISON IN TERMS OF SNR BETWEEN IM-DD AND OFM ROF SYSTEMS AGAINST SBS AT 50 KM FIBRE LENGTH.....	41
FIGURE 4-18 MEASUREMENT SET-UP USED TO DETERMINE THE SBS GAIN SPECTRUM.....	42
FIGURE 4-19 MEASURED SBS GAIN SPECTRA FOR THE IM-DD AND THE OFM ROF SYSTEMS FOR 25 KM SMF AND 20 MW INPUT POWER.....	43
FIGURE 4-20 SIMULATIONS AND MEASUREMENTS OF THE 5 TH HARMONIC FOR SWEEP FREQUENCIES BETWEEN 0.1 AND 7 GHZ, AT A FIBRE LENGTH OF 25 KM	44
FIGURE 4-21 SIMULATIONS AND MEASUREMENTS OF 5TH HARMONIC, F_M IS 4.4 GHZ FOR DIFFERENT FIBRE LENGTHS. MEASUREMENTS ARE DISPLAYED AS DOTS.....	45

TABLE 3-1 SIMULATION PARAMETERS	20
TABLE 4-1 LINK BUDGET AT HEADEND	31
TABLE 4-2 POWER BUDGET IN THE LINK.....	32
TABLE 4-3 LINK BUDGET FOR DIFFERENT FIBER LENGTHS	32
TABLE 4-4 IMPACT OF THE EDFA NOISE ON THE EVM	34

ABBREVIATIONS

AC	Alternating Current
ADSL	Asymmetric Digital Subscriber Line
AN	Access Node
APD	Avalanche Photo Diode
APON	ATM PON
ASIC	Application-Specific Integrated Circuits
ATM	Asynchronous Transfer Modulation
AWG	Arrayed Waveguide Grating
BER	Bit Error Rate
BPON	Broadband PON
BS	Base Station
B2B	Back to Back
BWDM	Band Wavelength Division Multiplexing
CAGR	Compound Annual Growth Rate
CATV	Cable Television
CEx	Central Exchange
CN	Central Node
CO	Central Office
CPE	Customer Premises Equipment
CWDM	Coarse Wavelength Division Multiplexing
DAS	Distributed Antenna System
DC	Directional Coupler
DMUX	Demultiplexer
DSB-LD	Distributed Feedback Laser Diode
DSL	Digital Subscriber Line
DSLAM	DSL Access Multiplexer
DWDM	Dense Wavelength Division Multiplexing
EDFA	Erbium Doped Fibre Amplifier
EFMA	Ethernet in the First mile Alliance
EN	Edge Node
EOL	End of life
EPON	Ethernet PON
ERD	European Rural Development
EVM	Error Vector Magnitude
Ex	Exchange
FDM	Frequency-division multiplexing
FEXT	Far End Crosstalk
FITL	Fibre In The Loop

FM-IM	Frequency Modulation-Intensity Modulation
FP	Flexibility Point
FRPP	Fast Ring Protection Protocol
FSAN	Full-Service Access Network
FTTB	Fibre to the Building
FSR	Free Spectral Range
FTTC	Fibre to the Curb
FTTCab	Fibre to the Cabinet
FTTH	Fibre to the Home
FTTN	Fibre to the Node
FTTP	Fibre to the Premises
FTTX	Fibre to X (includes all option)
FWA	Fixed Wireless Access
G _B	Growth in Bandwidth
GbE	Gigabit Ethernet
GDP	Gross Domestic Product
GPON	Gigabit PON
G _R	Growth in Revenue
HDSL	High bit-rate Digital Subscriber Line
HPF	High Pass Filter
IM-DD	Intensity Modulation with Direct Detection
ITU	International Telecommunications Union
JRC	Japan Radio Company
LE	Local Exchange
LOS	Line of Sight, Loss of Signal
LR-PON	Long Reach PON
MAC	Medium Access Control
MAP	Metro Access Points
MIMO	Multi Input Multi Output
MSAN	Multi Service Access Node
MUX	Multiplexer
NEXT	Near End Crosstalk
MZI	Mach-Zehnder Interferometer
NS2	Network Simulator 2
O/E	Optical/Electrical
OA	Optical Amplifier
OADM	Optical Add Drop Multiplexer
OFDM	Orthogonal Frequency Division Multiplexing
OFM	Optical Frequency Multiplication
OLT	Optical Line Termination
ONT	Optical Network Terminal

ONU	Optical Network Unit
OOK	On-Off-Keying
OSNR	Optical Signal to Noise Ratio
P2P	Point-to-Point
PCB	Printed Circuit Board
PDFA	Praseodym-Doped Fibre Amplifier
PIN	p – intrinsic – n layer
PIN-TIA	PIN Transimpedance
PLC	Planar Lightwave Circuit
PMD	Polarization Mode Dispersion, Physical Media Dependant
PON	Passive Optical Network
PSTN	Public Switched Telephone Network
QAM	Quadrature Amplitude Modulation
QoS	Quality of Service
RAM	Remote Access Multiplexer
RAU	Remote Antenna Unit
RF	Radio Frequency
RHD	Remote Heterodyne Detection
ROCE	Return on Capital Expenditure
RoF	Radio over Fibre
RSTP	Rapid Spanning Tree Protocol
RXT	Rayleigh Crosstalk
SAI	Service-Area Interface
SCM	Sub-Carrier Multiplexing
SBS	Stimulated Brillouin Scattering
SDH	Synchronous Digital Hierarchy
SDSL	Symmetric Digital Subscriber Line
SMF	Standard Single Mode Fibre (ITU-T G.652)
SOA	Semiconductor Optical Amplifier
SOHO	Small Office/Home Office
SPOF	Single Point of Failure
SRS	Stimulated Raman Scattering
TDM	Time Division Multiplexing
TDMA	Time Division Multiple Access
TFF	Thin-Film Filter
TRx	Transceiver
UTP	Unshielded Twisted Pair
VDSL	Very-High-Data-Rate DSL
VSDLoO	VDSL over Optic
VPI	Virtual Photonics Incorporated
WDM	Wavelength Division Multiplexing

WIPAS	Wireless IP Access System
WLAN	Wireless Local Area Network
WTU	Wireless Terminal Unit
xDSL	Some type (x) of DSL technologies
XL PON	XLarge – PON

1 INTRODUCTION

In the framework of the XL-PON node consolidation activities in the IST project MUSE, alternative ways to achieve node consolidation are developed. One of these alternatives is FWA based on RoF. A major property of a RoF system is that radio access points or base stations are significantly simplified through the consolidation of signal processing functions in the headend. In addition wireless access has the inherent advantage of being able to reach all users and FWA can be deployed in areas or buildings where it is difficult or impossible to deploy wired infrastructure (xDSL / fibre).

A cost-effective and WiMAX compliant solution to implement RoF to feed base stations for FWA was developed in Phase I as an alternative to the conventional digital baseband feeders deployed today. The employed system is based on the OFM method. OFM enables the use of only low-frequency optical components at the headend, while supporting high-frequency wireless system operation at the simplified Remote Antenna Unit (RAU). OFM involves the interferometric filtering of a FM optical signal and the resulting FM-IM conversion is used to optically up-convert carrier frequencies. The appearing high order harmonic components of the sweep frequency are used as a Radio Frequency (RF) carrier at the RAU [1].

Experiments have shown that OFM is chromatic dispersion tolerant, making it possible to have a much longer reach (> 10 times) than Intensity Modulation with IM-DD [2]. This tolerance is due to the sweeping of the optical wavelength: both the interferometric filtering and the chromatic dispersion will result in FM-IM conversion, which causes the generation of sweep frequency harmonics. Because of its dispersion tolerance OFM is very suitable for this study.

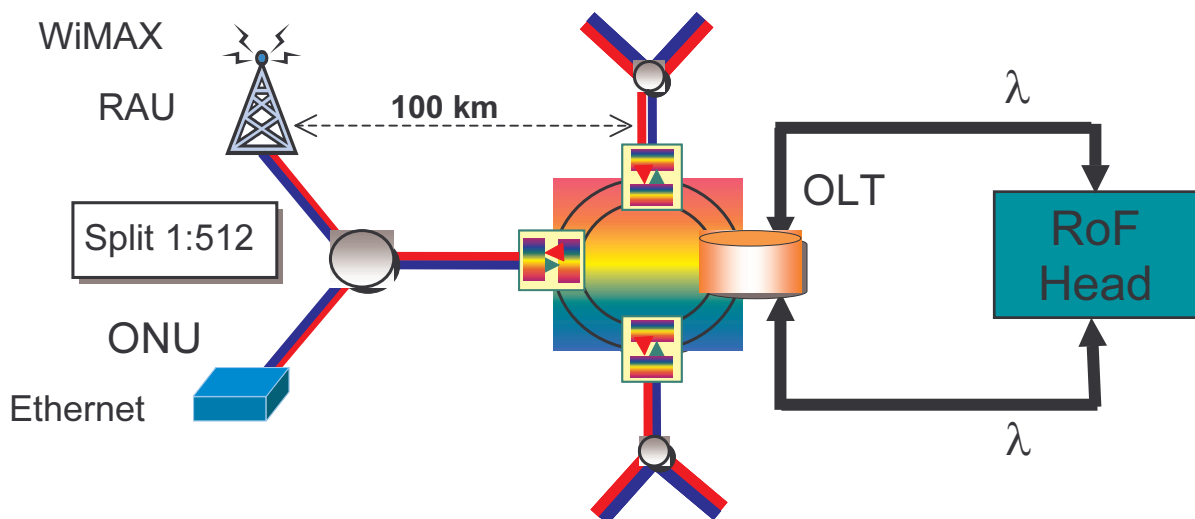


Figure 1-1 The XL PON with interconnected FWA feeder system

An implementation of the OFM system in the XL PON will require a separate wavelength overlay. Figure 1-1 shows how the system can be interconnected with the XL-PON. There are several issues regarding this interconnection which need to be considered. Of major importance is that the splitting factor and the reach of the PON system put constraints on the optical power budget in the FWA feeder network. It was, therefore, decided to investigate the ability of the RoF system to transport WiMAX compliant FWA services over a long optical link.

A challenging criterion is that the OFM system must be able to operate over fibre lengths up to 100 km. Additional non-linear effects in the fibre transmission link will have impact on the RoF system.

This report presents results on the dispersion characteristics of the OFM system, including experimental findings and theoretical work. A model has been developed, which describes the behaviour of the OFM system in the presence of chromatic dispersion. In the next sections it will be studied through measurements and simulations how the interferometric filtering and the fibre chromatic dispersion contribute to the generation of sweep frequency harmonics.

In long-reach optical fibre links it is desired to launch high power in order to offset the effects of the higher attenuation losses that occur along the fibre. However, increasing the launch power may lead to nonlinear effects taking place owing to the high optical intensity that may occur in the fibre core given the small core radius in standard SMF (Single Mode Fibre). Two such effects that occur when the optical power launched into the fibre exceeds a threshold level are the SBS, and the Stimulated Raman Scattering (SRS). Because the threshold level of SBS is generally much higher than that of SRS, SBS tends to limit the maximum power that may be launched into the fibre. For this reason, the effects of SBS in the OFM-based RoF system are investigated with experiments.

As optical amplifiers will be needed in the XL PON architecture to cover the fibre and splitter losses, the impact of ASE (Amplified Spontaneous Emission) on the RoF quality needs to be evaluated. Therefore, additional research is mandatory for such disturbances.

2 APPROACH

2.1 Overview

The operability of OFM using long fibre links will be studied with experiments and theoretical work. The objective in the theoretical activities is to support and comprehend the measurements on the fibre non-linearities and the optical link budgets.

The following approach will be adopted:

1. Model development
2. Model validation with measurements
3. Sensitivity analysis
4. Discussion on the results

The model will be validated for two scenarios:

- I. Different radio frequencies
- II. Different fibre lengths

Results from these simulations will be compared to simulations of a traditional IM-DD system.

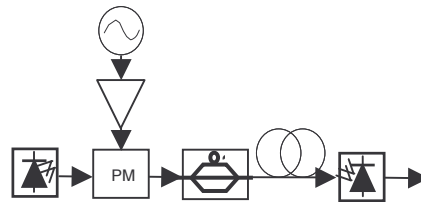


Figure 2-1 Basic scheme for the OFM model

Figure 2-1 shows the basic scheme that will be used in the modeling of the OFM system. It includes the main components which are necessary to achieve the optical up conversion process. A detailed description can be found in [1].

The next sections provide a theoretical background on dispersion characteristics of the OFM system. A model has been developed, which describes the behaviour of the OFM system in the presence of chromatic dispersion. First a model describing dispersion in an IM-DD system is outlined for the purpose of comparison. Secondly, a model for the OFM system including chromatic dispersion is presented. The last section provides an overview of the experimental work.

2.2 IM-DD Dispersion model

A simple model for IM-DD dispersion is given by the following expression for the output current of a photo detector (PD) which is illuminated with an IM optical signal [3]:

$$i_{out}(t) = 2R_d \sqrt{P_0} \left\{ 1 + \frac{1}{4} m^2 \cos^2 \omega_m (t - \beta_o'' L) + m \cos\left(\frac{1}{2} \beta_o'' L \omega_m^2\right) \cos^2 \omega_m (t - \beta_o' L) \right\} \quad (1)$$

where β_0' and β_0'' are respectively the 1st and 2nd derivative of the fibre's phase characteristic $f(\beta)$, L is the fibre length, R_d is the responsivity of the PD, P_0 is the optical power, ω_m is the angular frequency of the modulation signal, ω_0 is the angular frequency of the light wave and m is the modulation index. For small m it follows that $i_{out} \sim \cos(\frac{1}{2} \beta_0'' L \omega_m^2)$ so severe dips will occur at fibre lengths

$$L = \frac{(2k+1)\pi}{\beta_0'' \omega_m^2} \quad (2)$$

2.3 OFM Dispersion model

For the OFM processing a Mach Zehnder Interferometer (MZI) is assumed and it is shown in [3] that, after transmission over dispersive fibre the power of the n^{th} harmonic ($n = 1, 2, \dots$) is given by

$$P_n = A_n^2 + B_n^2 \quad (3)$$

where

$$A_n = \sum_{k=-\infty}^{\infty} J_k(\beta) J_{n-k}(\beta) \cos(\beta_0'' L \omega_m^2 n k) \times \left[\cos((\omega_0 + k\omega_m)\tau) - \cos\left(\frac{1}{2} n \omega_m \tau\right) \right] \quad (4)$$

$$B_n = \sum_{k=-\infty}^{\infty} J_k(\beta) J_{n-k}(\beta) \sin(\beta_0'' L \omega_m^2 n k) \times \left[\cos((\omega_0 + k\omega_m)\tau) - \cos\left(\frac{1}{2} n \omega_m \tau\right) \right]$$

with J_k the k^{th} order Bessel function of the first kind, β the FM index, ω_m the FM sweep frequency, ω_0 the optical carrier frequency, τ the differential arm delay of the MZI and

$$\beta_0'' = \frac{-D\lambda_0^2}{2\pi c} \quad (5)$$

with D the fibre dispersion parameter, λ_0 the wavelength of the optical carrier and c the speed of light in vacuum.

The impact of interferometric filtering and chromatic dispersion can be examined in more detail after unraveling the model given by (4). A further simplification is possible using Graf's addition formula (e.g. (4) in Watson, pp. 361 [4]):

$$J_n\left(\frac{\beta}{2} \sin\left(\frac{\zeta}{2}\right)\right) \frac{\cos(n\varphi)}{\sin} = \sum_{k=-\infty}^{\infty} J_{k+n}(\beta) J_k(\beta) \frac{\cos(k\zeta)}{\sin} \quad (6)$$

where $\beta \cos(\zeta) = \beta \cos(\varphi)$, and $\beta \sin(\zeta) = \beta \sin(\varphi)$. By combining (3), (4) and (6), and using trigonometric identities, it can be shown that:

$$P_n = \frac{1}{4} J_n(\beta_1)^2 + \frac{1}{4} J_n(\beta_2)^2 + J_n(\beta_3)^2 \cos(\omega_n) + (J_n(\beta_1) + J_n(\beta_2)) J_n(\beta_3) \cos(\omega_n) \cos(\omega_0 \tau) + \frac{1}{2} J_n(\beta_1) J_n(\beta_2) \cos(2\omega_0 \tau) \quad (7)$$

where

$$\begin{aligned}
 \beta_1 &= \beta/2 \sin\left(\frac{1}{2}(\beta_0'' L \omega_m^2 n + \omega_m \tau)\right) \\
 \beta_2 &= \beta/2 \sin\left(\frac{1}{2}(\beta_0'' L \omega_m^2 n - \omega_m \tau)\right) \\
 \beta_3 &= \beta/2 \sin\left(\frac{1}{2} \beta_0'' L \omega_m^2 n\right) \\
 \omega_n &= n/2 \omega_m \tau
 \end{aligned} \tag{8}$$

A first inspection of the model given by (7) learns that the power of the n^{th} harmonic is a summation of terms resulting from the interaction between dispersion and interferometric filtering. The third term (containing β_3) is equivalent with the power of an n^{th} harmonic which is generated by fibre dispersion only. A technique to generate RF signals in this way is reported in [5].

The model further shows that it is possible to optimize the power by tuning the optical carrier frequency with the MZI. The corresponding optical frequencies are the extremes of (7) with respect to ω_0 and are given respectively by:

$$\begin{aligned}
 \omega_{0,1} &= 2l \pi / \tau \\
 \omega_{0,2} &= (2l + 1) \pi / \tau \\
 \omega_{0,3} &= \pm 1 / \tau \cos^{-1} \left(- \frac{(J_n(\beta_1) + J_n(\beta_2)) J_n(\beta_3) \cos(\omega_n)}{2 J_n(\beta_1) J_n(\beta_2)} \right) + 2l \pi / \tau
 \end{aligned} \tag{9}$$

where l is an integer.

It is noted that the first two extremes $\omega_{0,1,2}$ correspond respectively, to the optical frequencies that maximize the generation of even and odd harmonics in the OFM system without the presence of dispersive fibre (e.g. [2]). When dispersive fibre is present these frequencies optimize both even and odd harmonics.

The presented model and derived expressions can serve to determine optimal operation parameters during experiments with the OFM system.

Dependence on fibre length

In order to gain insight in the dependence on fibre length it is necessary to determine when the power vanishes due to the cancellation of terms in (7). The following zeros for (7) can easily be found. Assume that:

$$\omega_m = \pi / \tau \tag{10}$$

then for the odd harmonics with $n = 2l+1$, (7) simplifies to:

$$P_{2l+1} = \left(J_{2l+1} \left(\frac{\beta}{2} \cos \left(\frac{1}{2} \beta_0'' L \omega_m^2 (2l+1) \right) \right) \sin(\omega_0 \tau) \right)^2 \quad (11)$$

Alternatively, assume that

$$\omega_m = 2\pi / \tau \quad (12)$$

then for the even harmonics with $n = 2l$, (7) simplifies to:

$$P_{2l} = \left(J_{2l} \left(\frac{\beta}{2} \sin(\beta_0'' L \omega_m^2 l) \right) (\cos(\omega_0 \tau) + 1) \right)^2 \quad (13)$$

The expressions given by (11) and (13) for the odd and even harmonics respectively, have an infinite number of zeros and show that in this case the FM-IM conversion is determined by chromatic dispersion. Therefore, the values for ω_m that are given by (10) and (12) should be avoided.

2.4 Experimental approach

Several laboratory experiments were conducted in order to verify the behaviour predicted by theory. In some cases, the experiments themselves were used to investigate the behaviour and the performance of the system. In many cases, experimental conditions as would apply to a practical system implementation were used to assess the realistic performance of the systems. As a reference, modulated signals complying with the single carrier WiMAX standard were used whenever the evaluation of the signal transmission quality was needed.

In order to make fair comparisons the behaviours and performances of IM-DD and OFM RoF systems, it was endeavoured to keep the operating points of all devices in the system the same as much as possible. For instance, to switch from the OFM system to the IM-DD system, the phase modulator would be left in the system and the sweep signal merely turned off, as opposed to disconnecting the phase modulator, which would change the operating parameters of any optical amplifiers immediately following.

Because of time constraints and availability of optical components, the measurements were limited to fibre lengths of 72 km. The experiments will be extended in a later stage to cover the XL-PON reach requirement.

3 THEORETICAL RESULTS

3.1 OFM dispersion model analysis

In the theoretical analysis of the dispersion impact on OFM, a sensitivity analysis is performed to assess the dispersion tolerance for the parameters frequency and fibre length using the model given by (7) in the previous chapter. This model is then further elaborated to understand the principle mechanisms behind the dispersion tolerance. The model will be examined for different frequencies and fibre lengths. Please refer to section 4.2 for validation results of (7) using experimental findings.

3.1.1 Sensitivity analysis

The performance of the OFM system in the presence of dispersive fibre follows from a comparison with results using an IM-DD scheme. Table 3-1 lists the involved simulations parameters.

Table 3-1 Simulation parameters

Approach for variable f	Approach for variable L
Change f in IM between 1 – 38 GHz to determine “nulls” in 25 km of SMF Performance using OFM scheme (by varying sweep frequency 1 – 7 GHz; while keeping β constant) $\beta \sim 3.3$ Dispersion parameter ~ 16.2 ps/nm km FSR ~ 10 GHz $\lambda \sim 1550$ nm $L \sim 25$ km	Change L in IM between 0 – 100 km to determine “nulls” f in IM ~ 23 GHz Performance using OFM scheme (by varying L between 0 – 100 km) $\beta \sim 3.3$ Dispersion parameter ~ 16.2 ps/nm km FSR ~ 10 GHz $\lambda \sim 1550$ nm sweep frequency ~ 4.44 GHz $\omega_m = 2\pi f_m$

Simulations were performed with the parameters given by Table 3-1 by changing the sweep frequency and fibre length. The following figures show the results from these simulations.

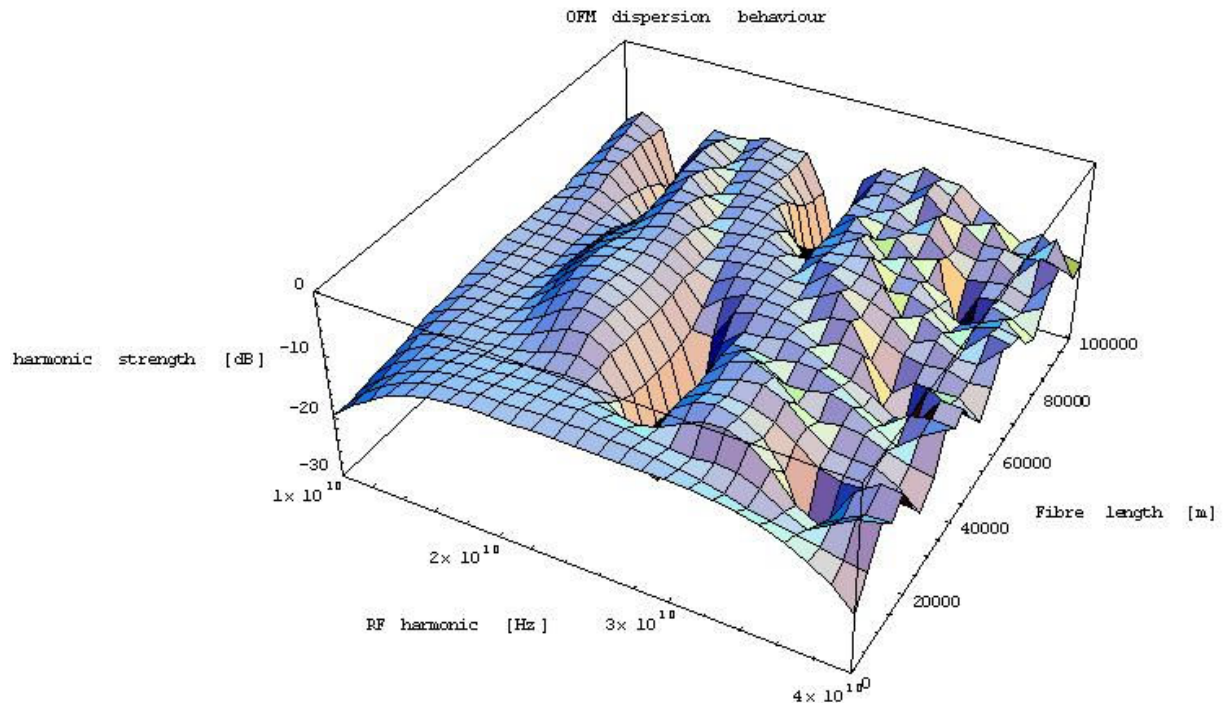


Figure 3-1 OFM dispersion behaviour (5th harmonic)

Figure 3-1 shows a 3-dimensional plot, where the RF (5th harmonic of the sweep frequency) is ranging from 1 to 40 GHz. The fibre lengths in the simulations ranged from 0 (B2B) to 100 km. It can be seen that there are strong but mostly local variations, because from 10 – 25 GHz the behaviour is rather smooth. Also a “hill” is present around 25 GHz, a closer examination reveals that this phenomenon is a FM-IM conversion gain due to fibre dispersion (please refer to section 4.2 for more details). Above 30 GHz larger fluctuations are found when the fibre length is varied, indicating a growing impact of dispersion at these ranges.

Although fibre dispersion has an impact on the OFM simulations Figure 3-1 clearly illustrates the dispersion tolerance of OFM when compared with the next plot.

Figure 3-2 is a 3D plot of the strength of an intensity modulated optical signal for modulation frequencies 1 – 40 GHz and fibre lengths 0 (B2B) – 100 km, which was obtained using (1) and the parameters given in Table 3-1. Very strong fluctuations are present. The large number of fringes illustrates the strong effect of fibre dispersion in IM systems.

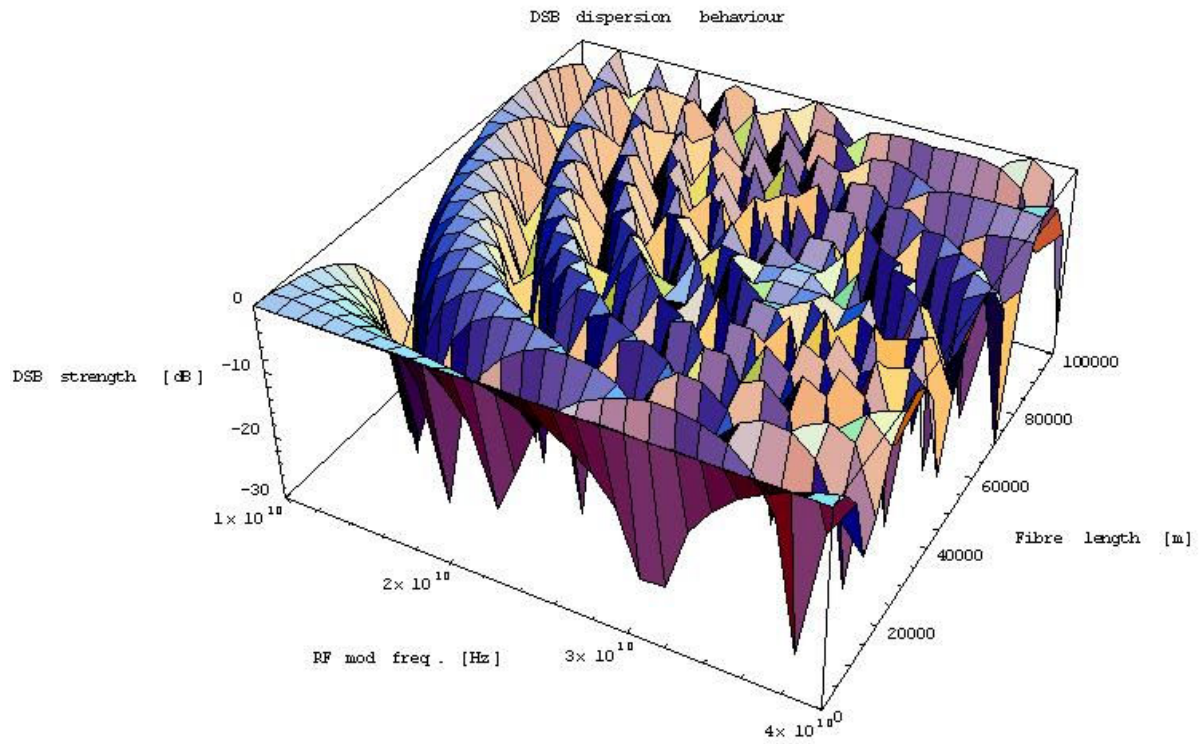


Figure 3-2 IM-DD dispersion behaviour

The comparison of the OFM and IM-DD results clearly shows that OFM is superior over IM-DD regarding their performance in the presence of chromatic dispersion.

3.1.2 OFM chromatic dispersion tolerance

In this section the dispersion tolerance of OFM is further examined. From the sensitivity analysis it became apparent that the dispersive fibre has an impact which is due to the additional FM-IM conversion. To illustrate this further simulations have been performed with harmonics suppressed by biasing the optical frequency with the MZI.

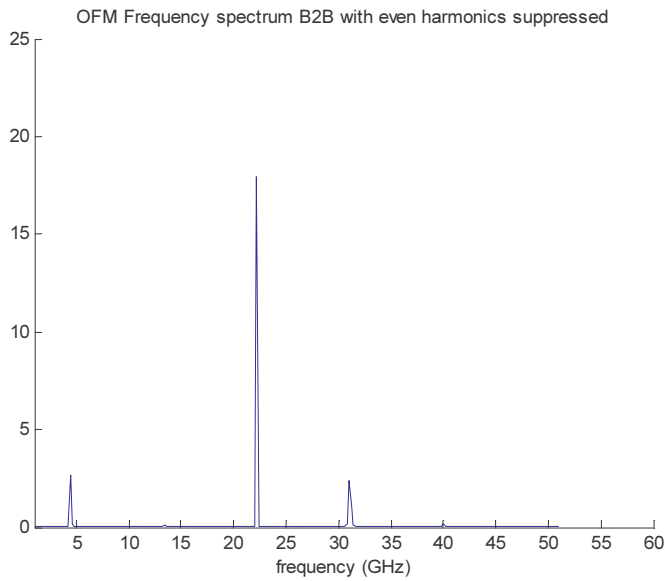


Figure 3-3 OFM frequency spectrum (with the even harmonics suppressed) in B2B configuration

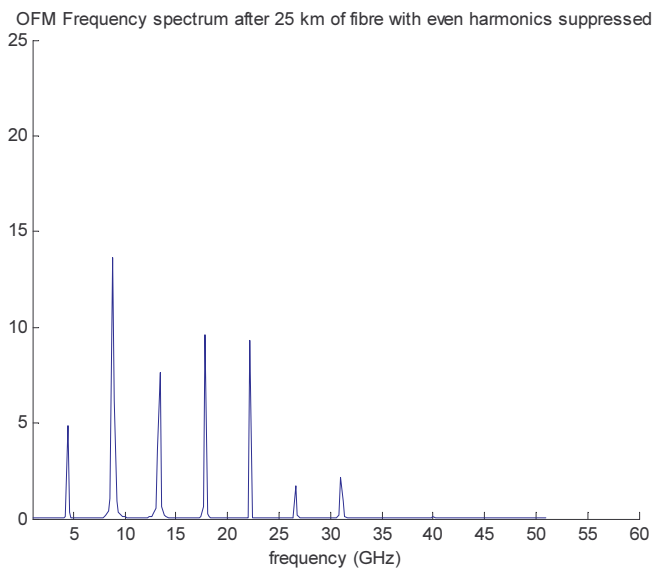


Figure 3-4 OFM frequency spectrum (with the even harmonics suppressed) after 25 km of SMF

Figure 3-3 shows the B2B spectrum at the PD with the even harmonics suppressed. Only the 1st, 5th and 7th harmonic can be observed. The effect of the dispersive fibre manifests itself in Figure 3-4. Here 25 km of fibre is inserted and now even harmonics are present in the spectrum, which is caused by additional FM-IM conversion by the dispersive fibre.

The OFM model together with VPItransmissionMaker simulations were used to investigate the influence of OFM system parameters on its behavior. The simulations were based on Figure 2-1 and Table 3-1. The two parameters, which could be varied in the experiments, namely the frequency modulation index and the filter biasing, were both found to influence the profile of the actual signal amplitude variation with fibre length (see section 4.1). For instance, the sensitivity of the OFM system to filter biasing (when chromatic dispersion is present) is given in Figure 3-5. In this case the laser wavelength was varied by 2 GHz on either side of the optimal (for the odd harmonic) back-to-back biasing, which was at the halfway point between the maximum and the minimum transmission of the filter, in this case at 2.5 GHz.

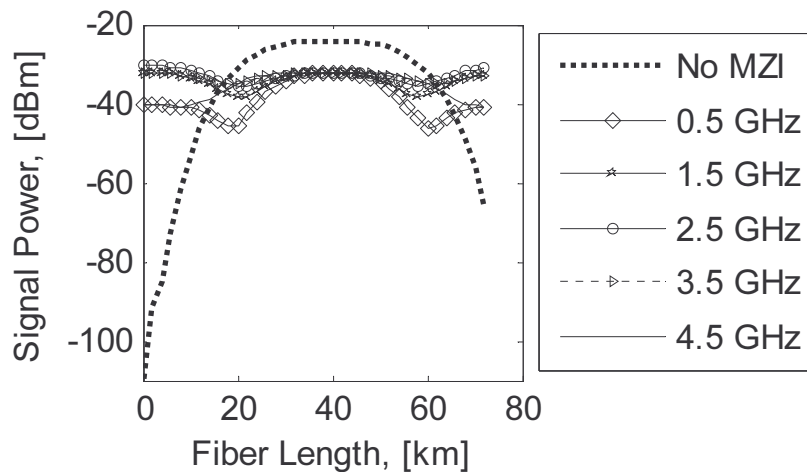


Figure 3-5 Influence of MZI filter biasing on the behavior of the OFM system

It was observed that the optimal biasing of 2.5 GHz, produced the least variation (< 3 dB) in the signal strength, but resulted in no gain (when compared with the back-to-back signal power). In contrast, biasing the filter further away from the optimal value resulted in a lower back-to-back RF power and a power gain for fiber lengths between 20 km and 50 km. To help explain this behavior, an additional curve for the case when the MZI was removed from the OFM system is also plotted in Figure 3-5. Thus, this curve represents the dispersion-induced FM-IM conversion gain. It again clearly demonstrates the advantage of OFM over dispersion-induced FM-IM conversion, whose conversion gain exhibits severe fiber length dependence as shown.

Simulation results using (7) provide additional insight in the contributions to FM-IM conversion of both the interferometric filter and chromatic dispersion. For convenience the first two interaction terms in (7) are combined as:

$$t1 = \frac{1}{4} J_n(\beta_1)^2 + \frac{1}{4} J_n(\beta_2)^2 \quad (14)$$

$$t2 = (J_n(\beta_1) + J_n(\beta_2)) J_n(\beta_3) \cos(\omega_n) \cos(\omega_0 \tau) + \frac{1}{2} J_n(\beta_1) J_n(\beta_2) \cos(2\omega_0 \tau) \quad (15)$$

Figure 3-6 depicts the three interaction components and P_n for fibre lengths between 0 and 100 km for the 5th harmonic, where the dispersion term refers to the third term in (7). In the simulations the parameters given by Table 3-1 were used and there was no biasing of the optical carrier with the filter.

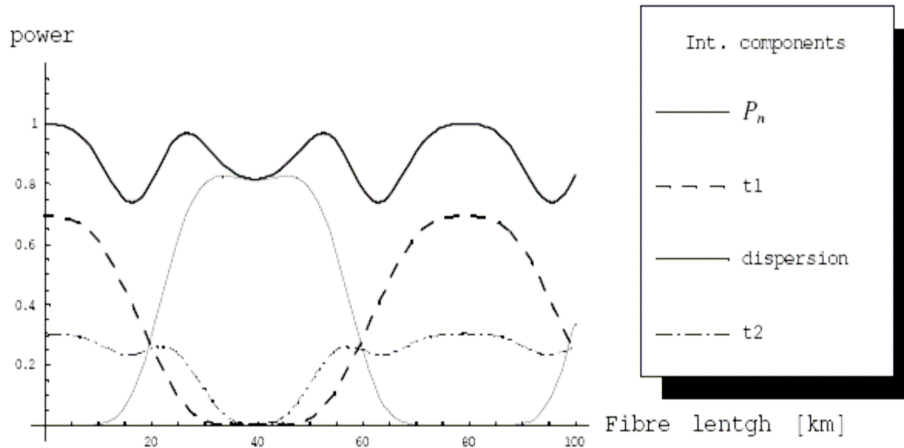


Figure 3-6 Simulated interaction components of 5th harmonic, f_m is 4.4 GHz for different fibre lengths

From Figure 3-6 it can be observed that both the interferometric filtering and the fibre chromatic dispersion contribute to the generation of sweep frequency harmonics. Between fibre lengths of 20 and 60 km the dispersion term dominates, outside this region the interaction between the interferometric filtering and the dispersion is the strongest. Apparently, the dispersion tolerance ensues from the presence of the other interaction terms which do not vanish at fibre lengths where the dispersion term exhibits strong dips. There is also symmetry around $L \sim 40$ km, which corresponds to the extreme for $J_n(\beta_3)$. The variation in the power is less than 3 dB which illustrates the small dependence on fibre length for the applied system parameters.

3.2 Discussion

The employed model, describing the behaviour of the OFM system in the presence of chromatic dispersion, allows for several conclusions.

It is observed that both the interferometric filtering and the fibre chromatic dispersion contribute to the generation of sweep frequency harmonics.

The model shows that OFM does not exhibit fading at certain fibre lengths as is the case with FM-IM conversion due to chromatic dispersion only. The dispersion tolerance ensues from the presence of the other interaction terms which do not vanish at these fibre lengths. It is noted however, that fading can occur in the OFM system for sweep frequencies given by (10) and (12) or an integer multiple of these values for respectively odd and even harmonics. In these specific cases all components are determined by chromatic dispersion. Therefore, the associated sweep frequencies are not to be used in an operational OFM system.

The presented model and derived expressions can serve to determine optimal operation parameters during experiments with the OFM system.

4 EXPERIMENTAL RESULTS

4.1 Experiments

4.1.1 Dispersion impact assessment

In order to experimentally determine and compare the impact of chromatic dispersion on the OFM and the IM-DD systems, the laboratory set-up given in Figure 4-1 was used. To make a valid comparison between the two systems, the operating parameters of the system devices were kept identical as much as possible. During IM-DD system measurements the phase modulator (PM) was not used (i.e. sweep signal was disabled) but returned in the set-up. In addition, the MZI was removed from the set-up and its insertion loss compensated for by the attenuator. Similarly, during the OFM system measurements, the intensity modulator (IM) was not used (i.e. switched off), but left connected in the set-up.

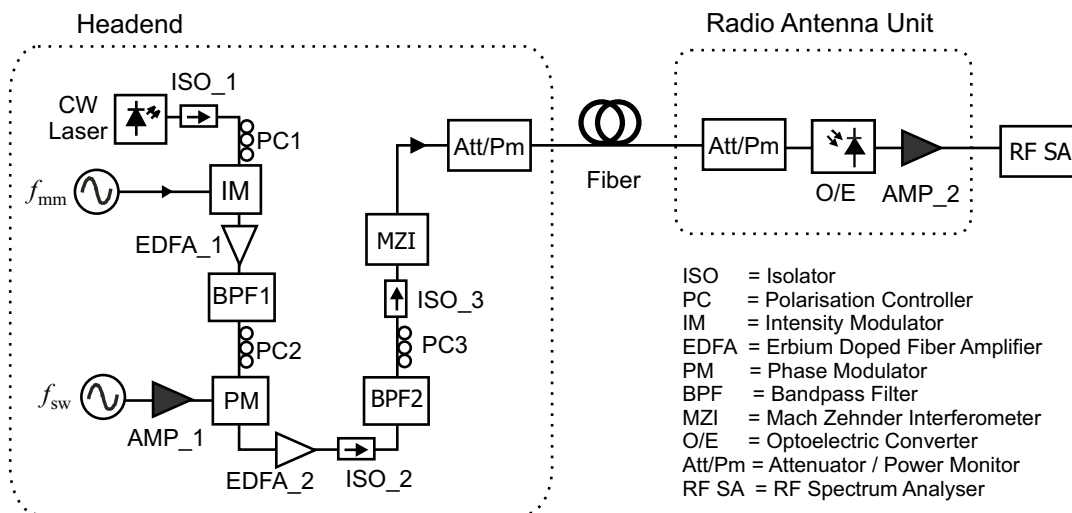


Figure 4-1 Laboratory set-up for measuring the impact of chromatic dispersion on the IM-DD and the OFM RoF systems.

The CW laser source was a DFB laser emitting optical power at $\lambda_0 = 1558.98$ nm. The Agilent 83650L signal generator was used as the source of the RF signals. The MZI was fibre-based and had a FSR = 10 GHz. It was kept in a box to insulate it from the outside environment.

After transmission over variable fibre lengths, the optical signal was fed into the simplified remote RAU consisting only of a photodetector (u2t Photonics, bandwidth = 38 GHz) and a LNA (SHF 806E, bandwidth = 38 GHz, gain = 26 dB). A variable attenuator was used to keep the detected optical power constant. The FSQ40 spectrum analyzer was used to measure the power of the received RF signal. The same RAU was used in both the IM-DD and the OFM experiments.

A. Measured Impact of Dispersion

For the IM-DD measurements the RF signal, $f_{mm} = 22.2$ GHz was applied to the IM, and its modulation depth adjusted so as to generate an RF signal of comparable power to the OFM-generated signal. Then, varying lengths of standard single-mode fibre (SMF) up to 72 km were inserted in between the headend and the RAU, and the corresponding power of the remotely-generated RF signal was recorded. The result is shown in Figure 4-2.

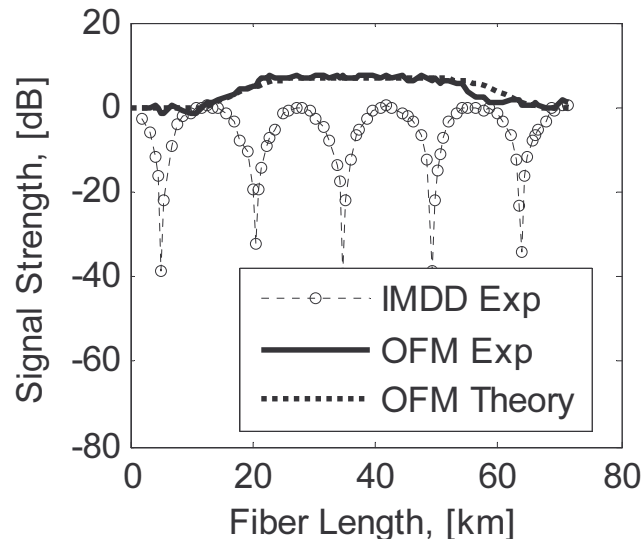


Figure 4-2 Measured impact of chromatic dispersion on IM-DD and OFM RoF systems, including the theoretical prediction for OFM.

Severe fading was observed at fibre length intervals of about 15 km, in line with the theoretical prediction. The maximum link length of the IM-DD system was less than 5 km as shown in Figure 4-2. Fluctuations in the fibre losses were eliminated from the measurements by using the attenuator to maintain the power received at the RAU at -12 dBm.

For the OFM RoF system measurements, it was necessary to first set a reasonable operating point of the system, before transmission over fibre. As stated earlier, several factors influence the intensity of the OFM-generated harmonic components. These factors include the frequency modulation depth, β , the relationship between the sweep frequency, f_{sw} ($= f_m$) and the filter's FSR, and the biasing of the filter (positioning the CW peak laser wavelength with respect to the transmission response of the filter). There was no optimization necessary for the sweep signal frequency-FSR relationship since the FSR of the MZI was fixed at 10 GHz, while the target frequency at the RAU of $f_{mm} = 22.2$ GHz, dictated a sweep signal frequency $f_{sw} = 4.44$ GHz, targeting the 5th harmonic. Therefore, β and the biasing of the filter were adjusted in order to produce a reasonably strong (≈ -60 dBm) signal at 22.2 GHz. Afterwards, varying lengths of SMF fibre were connected between the headend and the RAU, and the power of the generated signal recorded just as was done in the IM-DD case. The measurements were repeated several times over several days to make sure that they were repeatable.

Figure 4-2 also depicts the measured impact of chromatic dispersion on the OFM system. It was observed that in contrast to the IM-DD system, the OFM system showed no fading over the whole range of fibre lengths up to 72 km. In fact, a gain of about 6 dB was observed for fibre spans ranging between 20 km and 50 km. This result was in line with the theoretical prediction, which showed no fading in the OFM system. The source of the observed gain is discussed in section 4.2.

B. Quality of Transmitted Signals

OFM has already been shown to generate very pure signals of very narrow linewidth. In order to assess the quality of the OFM-transported signals, the phase noise of the signals was measured for different fibre lengths. No change in phase noise was observed. Furthermore, the OFM system was used to transport and up-convert a 100 Mbps, 16-QAM modulated sub-carrier signal from $f_{sc} = 200$ MHz to around 22.2 GHz as shown in Figure 4-3. After transmission over 50 km of SMF fibre, the Error Vector Magnitude (EVM) of the data recovered from the LSB was measured and found to be 4.9%, which is below the 6% (with coding) required for the single-carrier WiMAX standard. A clean constellation diagram was also obtained, as shown in Figure 4-3. The measured SNR was 26.1 dB.

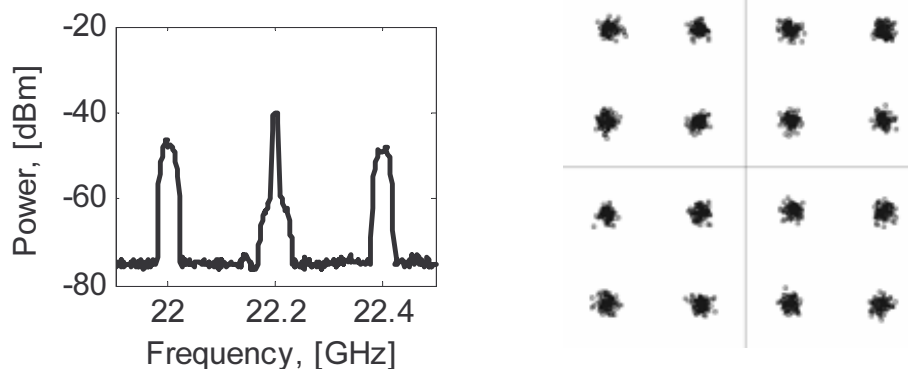


Figure 4-3 Spectrum of an OFM up-converted sub-carrier and constellation diagram of the 100 Mbps 16-QAM @ 22.4 GHz data recovered after transmission on 50 km SMF

The OFM system was also used to transmit a 16 QAM signal at 100Mbps with $f_{sc} = 1.5$ GHz at the frequency of 39.9 GHz (using in that case a sweep frequency of $f_{sw} = 6.4$ GHz and targeting the 6th harmonic) as shown in Figure 4-4. In this case, after the 50 km of SMF fiber, the EVM measured at the reception was 4.86%, still below the required 6%, and obtaining once again a clear constellation diagram, as shown in Figure 4-5 .

These results confirmed the high-quality transmission of 100 Mbps 16-QAM signals over long SMF lengths at frequencies up to 39.9 GHz. Therefore, OFM supports the distribution of high quality multi-standard, multi-frequency signals over flexible and extended SMF fibre lengths and high frequencies.

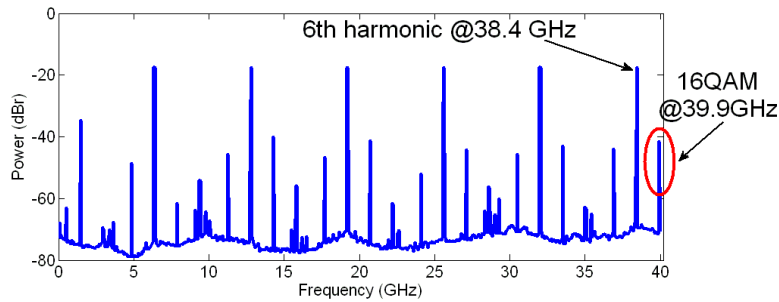


Figure 4-4 Spectrum of an OFM up-converted sub-carrier of the 100 Mbps 16-QAM @ 39.9 GHz data recovered after transmission on 50 km SMF

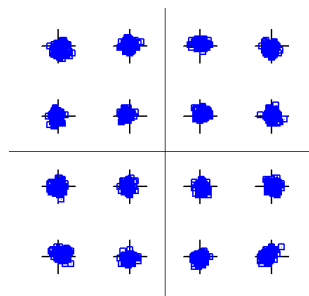


Figure 4-5 Constellation diagram of the 100 Mbps 16-QAM @ 39.9 GHz data recovered after transmission on 50 km SMF

4.1.2 OFM link loss budget

The optical link budget of OFM-based RoF systems identifies how far a signal can travel through the fibre from the headend side to the remote antenna units with an acceptable quality at the receiver before the signal needs to be corrected, or compensated for. The budget is consumed by the fibre attenuation plus the insertion loss of all connections, and the loss of components and the splices in the link.

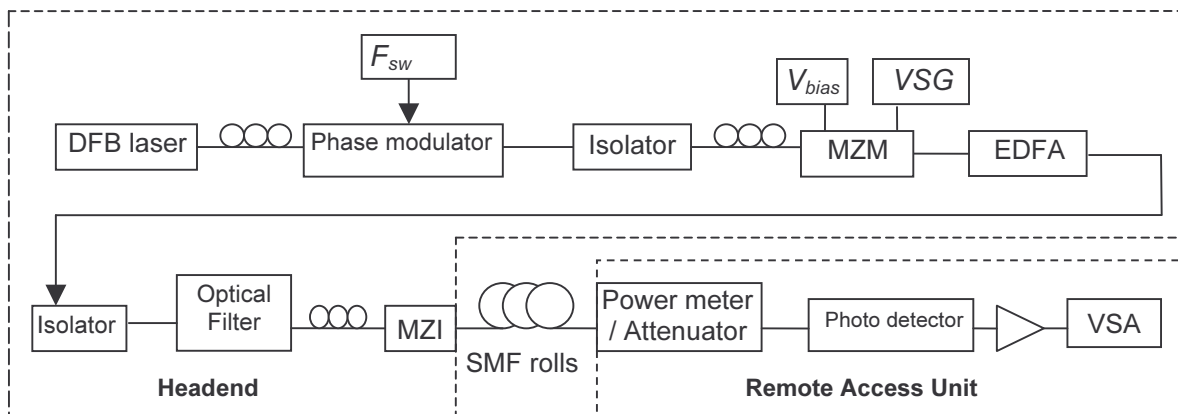


Figure 4-6: Measurement set-up for the OFM link loss budget

The assessment of the OFM link loss budget was conducted as in Figure 4-6. At the headend, the 5.48 dBm CW light emitted by the DFB laser at 1559 nm was sinusoidally swept by an optical phase modulator (PM). The PM was driven by a 4.4 GHz RF signal, and the output was then intensity modulated by a Mach Zehnder Intensity Modulator (MZM) driven by a 16 QAM modulated IF signal at 800 MHz with a bit rate of 100Mbps. The driving signal was produced by a vector signal generator (VSG). The resulting signal was optically amplified by an EDFA, and fed into a custom made Mach Zehnder Interferometer (MZI). The MZI was a 10 GHz free spectral range (FSR). The output of the MZI was transmitted over a standard single mode fiber with various lengths to the remote access unit, and finally analyzed by a vector signal analyzer (VSA).

Because the remote antenna unit in the OFM system is significantly simplified to have only a photodetector and an electrical signal amplifier, the budget becomes an important issue due to more connections at headend and longer lengths of the fiber.

The result of the link budget measurement at headend is shown in Table 4-1. The total loss of the headend is around 19.44 dBm which is mainly caused by the insertion loss and attenuations of the components in the link. Three main power-consumptive devices in the link, i.e, Mach-Zehnder intensity modulator, phase modulator, and Mach-Zehnder interferometer have a loss of 15.03 dBm, which accounts to the 77% of the total loss of the headend.

Components	Ports	Power (dBm)	Loss (dB)	Gain (dB)
1558.9 nm DFB laser	output	5.48		
Polarization Controller 1	input		-1.05	--
	output	4.43		
Phase Modulator	input		-4.41	---
	output	0.2		
Isolator 1	input		-1.2	--
	output	-1		
Polarization Controller 2	input		--	+0.17
	output	-0.83		
Intensity Modulator	input		-6.62	--
	output	-7.45		
* C-band EDFA	input		--	(a) +23.45 (b) +28.75
	output	(a) 16 (b) 21.3		
Isolator 2	input		-1.1	---
	output	(a) 14.9 (b) 20.2		
Optical filter	input		-1.4	---
	output	(a) 13.5 (b) 18.9		
Polarization Controller 3 Mach-Zehnder interferometer	input		-4	---
	output	(a) 9.5 (b) 14.9		
Total	---	---	-19.44	(a) 23.62 (b) 28.92

Table 4-1 Link budget at headend

* EDFA output (a) for 25 km and 50 km fiber measurements; (b) for 75 km and 100 km measurements

The loss in the fiber link (around 0.25 dbm / km) is constant, comprising the fiber and connector losses. Table 4-2 shows the loss budget and the system performance for various fiber lengths.

Fiber Length (km)	Power ejected into the fiber (dBm)	Power out of the fiber (dBm)	Received Power at photodetector (dBm)	Losses in the fiber and connectors (dBm)	EVM (%)	S/N (dB)
0 (back to back)	0	0	-3	0	4.7	26.5
25	9.5	3.2	-3	-6.3	5	26
50	9.5	-1.8	-3	-11.3	4.5	26.9
75	14.9	-6	-6	-20.9	4.8	26.4
100	13.85	-10.5	-10.5	-24.5	7.9	22

Table 4-2 Power budget in the link

An optical amplifier compensating for parts of these losses is required to achieve a good signal at the remote access unit. In the experiment, we employed an EDFA with two different outputs, (a: maximum 16 dBm output used in 25 km and 50 km cases, b: maximum 24 dBm output used in 75 km and 100 km cases). A large output power is desired for overcoming the high attenuation loss along the fiber. However, increasing the launch power into the fiber may increase nonlinear effects, and decreasing the RoF system performance. The fiber nonlinear effect will be discussed in section 4.1.4.

We measure the quality of transmitted signals for optimizing the launch power for the different fiber lengths. A back to back system measurement with an EVM at 4.7% and signal to noise ratio (S/N) at 26.5 dB is taken as a reference value. An optical attenuator is used before the photodetector to limit the detection power within the operation safety.

fiber length	25 km	50 km	75 km	100 km
Total loss	25.7 dB	30.7 dB	40.3 dB	43.9 dB
Power budget	3.36 dBm	-1.64 dBm	-6 dBm	-10.5 dBm
Power margin	6.36 dB	1.36 dB	0	0

Table 4-3 Link budget for different fiber lengths

Table 4-3 shows the experiment values of the total loss, power budget, and power margin of the OFM based RoF system. The total loss can be regarded as a summed loss of the headend and fiber. The power budget, P_{budget} , can be calculated according to following formula:

$$P_{budget} (dBm) = P_{transmitter} (dBm) + G (dB) - L_{headend} (dB) - L_{fiber} (dB), \quad (16)$$

where the $P_{transmitter}$ is the lasing power from the DFB laser, G is the gain, and L is the loss. The power margin is the power budget plus the power which have been adjusted by the attenuator for the safety reason.

4.1.3 Impact of EDFA noise

The EDFA (erbium doped fiber amplifier) is an important component of the OFM based RoF system because of the relatively losses imposed by the modulator in the transmitter and the FM to IM conversion in the periodic MZI structure. Apart from the optical gain which is desired effect, EDFA's will also introduce optical noise to the signal, which is considered an undesired effect.

The ASE (amplified spontaneous emission) noise appears at the output of the amplifier because of the spontaneous emission of the gain medium into the amplified mode.

The spontaneous emission power at the output from an optical amplifier is given by the following equation:

$$P_{sp} = N_{sp} (G-1) h\nu B_0 \tag{17}$$

Where N_{sp} is the spontaneous emission factor, G is the gain, h is Planck's constant, ν the optical frequency and B_0 is the optical bandwidth.

As showed in (17), we can observe that the noise is proportional to the gain of the EDFA and the optical bandwidth. This relation indicates that the maximum gain of the amplifier can be limited by the ASE noise, when the input signal is not strong enough.

A solution to this unwanted effect is the introduction of an optical band pass filter following the EDFA therefore maximum noise as possible can be eliminated.

In order to study the impact of the ASE noise in the system, some measurements were taken according to the setup in Figure 4-7. A tunable attenuator was placed in front of the EDFA to adjust the input power. After the EDFA we switched an optical band pass filter with 1 nm bandwidth between on and off to compare the optical spectrums and the corresponding signal quality in terms of EVM at VSA. The experiment was done in a back-to-back link. Data were modulated at 22.8 GHz with a QAM 16 scheme of 100 Mbit/s.

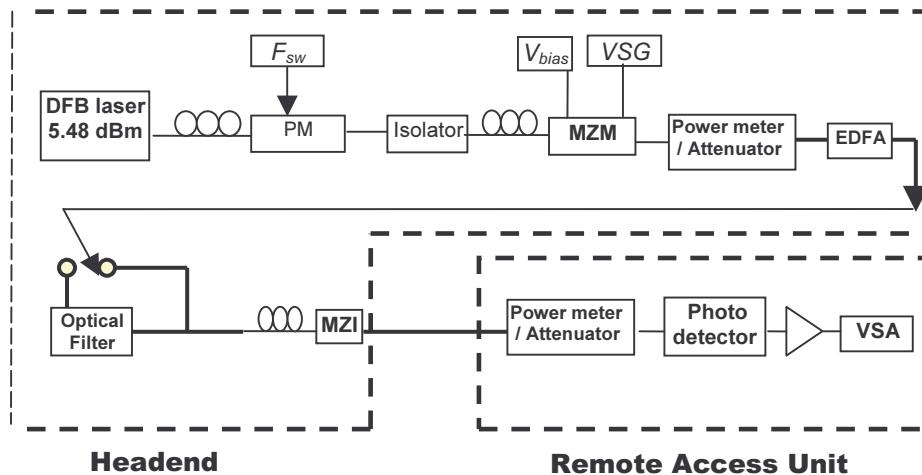


Figure 4-7 Experiment set-up for EDFA ASE noise assessment

The observed output optical spectrums of the EDFA in two cases, with and without presence of filter, are shown as below. In Figure 4-8, the comparison was performed at -19.5 dBm of the EDFA input power while -10.5 dBm in Figure 4-9.

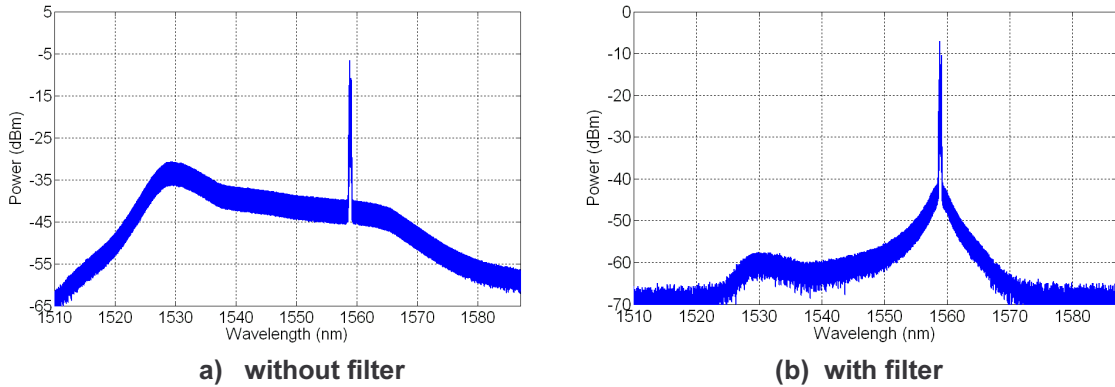


Figure 4-8 Optical spectrums comparison with EDFA input power at -19.5 dBm

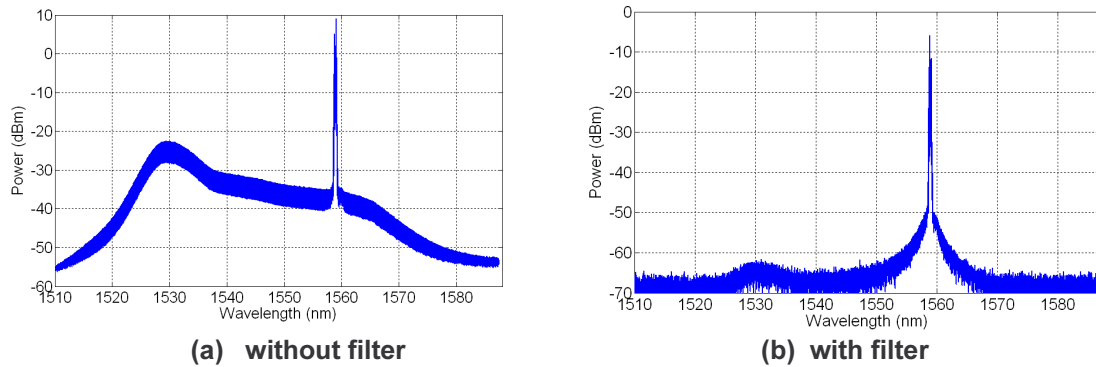


Figure 4-9 Optical spectrums comparison with EDFA input power at -10.5 dBm

Table 4-4 shows the impact of the EDFA noise on the system performance. From the contrasts of the spectrums in Figure 4-8 and Figure 4-9, the ASE noise was removed obviously by making use of filtering. However, if we contrast the system performance by means of EVM value, they show quite different results.

EDFA input (dBm)	EDFA output (dBm)	Gain dB	EVM (%) with filter	EVM (%) without filter
-19.5	7.2	26.7	5.6	10
-16	17.2	33.3	5.3	7.3
-10.5	20	30.5	5	5

Table 4-4 Impact of the EDFA noise on the EVM

When the input power to the EDFA is weak, at -19.5 dBm, (Figure 4-8), the EVM appears to be much better; 5.6 % in case of using a filter compared to 10 % in case of without filtering. However, when the EDFA input power increases (Figure 4-9), correspondingly, the optical signal noise ratio (OSNR) grows too. It makes the difference of system performance between the presence and absence of the filter decrease. Especially, while the input to the EDFA increases by -10.5 dBm, though the spectrum of the signal after filtering in Figure 4-9b looks better than Figure 4-9a, the OSNR value in Figure 4-9a is good enough and the EVM values registered in the vector analyzer indicates no difference at all in both cases (with and without the filter), about 5%.

According to our link budget experiment, the real input power to the EDFA is around -7.5 dBm, in that case, the presence of a filter in the system in order to limit the ASE noise is not necessary since the performance is the same.

4.1.4 Impact of non-linearities

In long-reach optical fibre links it is desired to launch high power in order to offset the effects of the higher attenuation losses that occur along the fibre. However, increasing the launch power may lead to nonlinear effects taking place owing to the high optical intensity that may occur in the fibre core given the small core radius in standard SMF. Two such effects that occur when the optical power launched into the fibre exceeds a threshold level are the Stimulated Brillouin Scattering (SBS), and the Stimulated Raman Scattering (SRS). Because the threshold level of SBS is generally much higher than that of SRS, SBS tends to limit the maximum power that may be launched into the fibre. For this reason, the effects of SBS in the OFM-based RoF system were investigated.

Stimulated Brillouin Scattering (SBS), occurs when optical power gets efficiently converted from the input pump power to the scattered stokes wave. The stokes wave propagates in the direction opposite to the pump signal. In addition, the scattered wave is also frequency-downshifted by about 10 GHz. The transfer of power from the pump signal into the stokes wave leads to the depletion of the pump signal. Once the SBS threshold is exceeded, most of the additional optical power ends up being transferred into the back-scattered signal. This imposes a limit on the maximum optical power that may be delivered to the other end of the optical fibre link. In addition, the forward-propagating scattered signal may affect the SNR performance of the link.

Impact of modulation depth on the SBS threshold

The OFM-based RoF system involves the phase of frequency modulation of the optical system followed by periodic filtering. Since the SBS gain spectrum is a function of the optical signal linewidth and the applied modulation scheme, it is expected that the FM modulation depth of the OFM system will have an impact on the SBS threshold level. In order to investigate this impact, the measurement set-up shown in Figure 4-10 was used. The wavelength of the laser was 1558.98 nm and its emitted power +3 dBm.

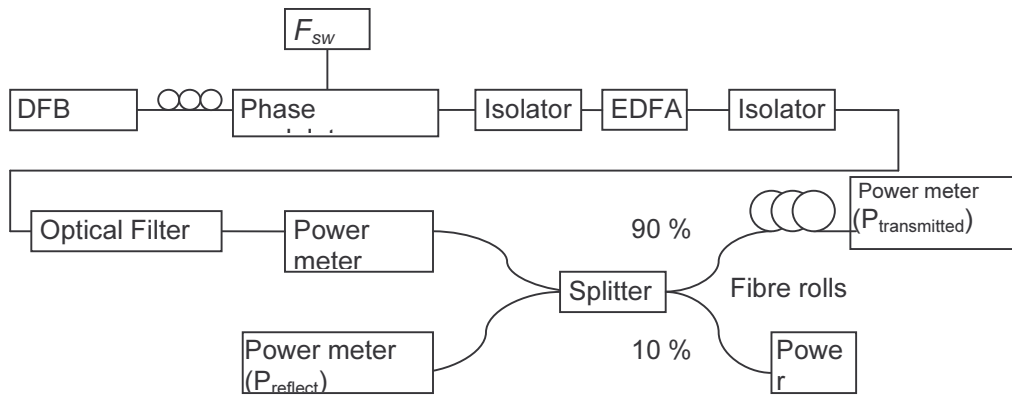


Figure 4-10 Measurement set-up for the impact of modulation depth on the SBS threshold

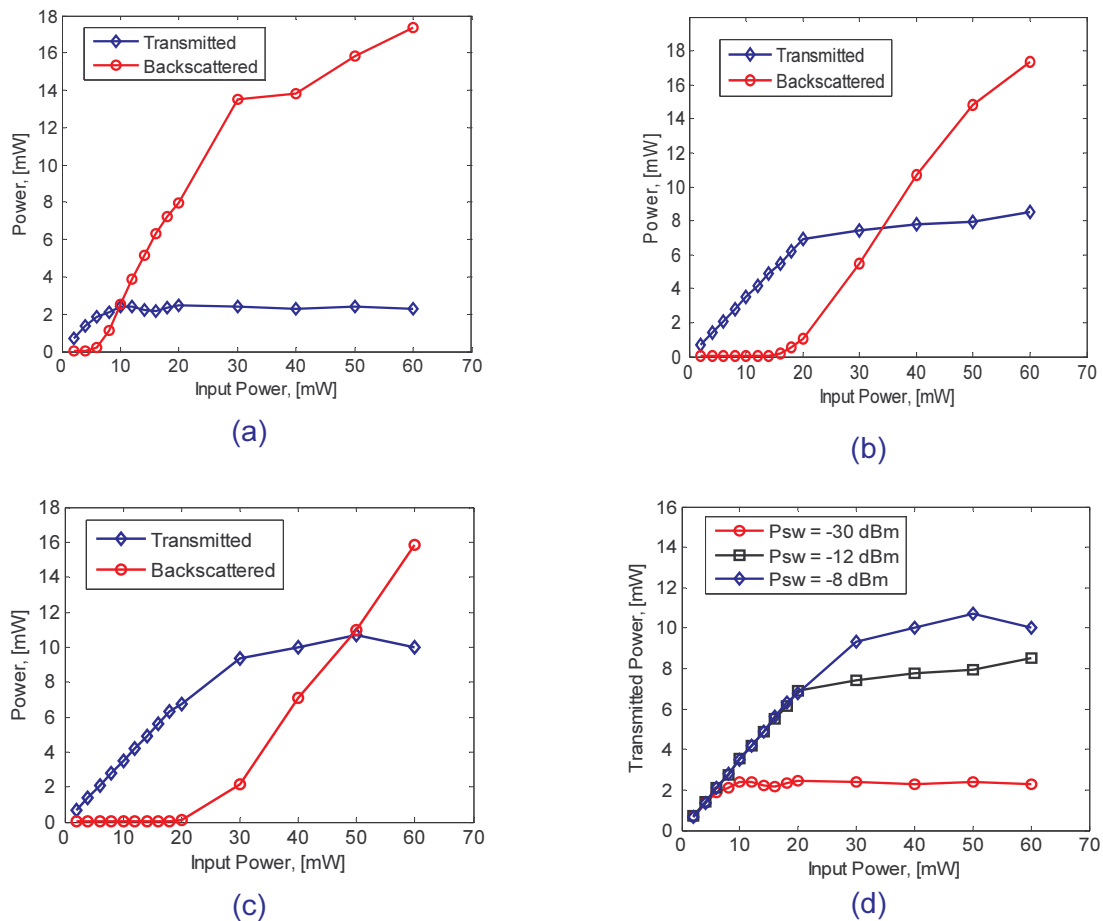


Figure 4-11: Measured impact of Phase Modulation depth on the SBS threshold value for sweep power equals (a) -30 dBm, (b) -12 dBm, (c) -8 dBm, and (d) comparison

The measured results for a fibre length equal to 25 km given in Figure 4-11 showed that a larger modulation depth resulted in a higher SBS threshold value. Figure 4-11 (a) corresponds to a normal IM-DD link with no modulation on the optical carrier. In that case the SBS threshold was about 10 mW. The threshold was raised to 50 mW for the case when the sweep signal drive power was equal to -8dBm. The increased threshold power is due to the broadened spectrum.

The implication of the variation in the SBS threshold is shown in Figure 4-11 (d), where the three cases are compared. In the figure, the power delivered at the end of the optical link is considered. It is observed that the higher FM index leads to more power being delivered at the end of the fibre link. A normal IM-DD system cannot deliver more than 2 mW at the end of a 25 km fibre link. However, an OFM system is capable of delivering 9 mW. These results show that an OFM-based RoF system can deliver more than 6dB more power than an IM-DD system for a 25 km fibre link.

Impact of Fibre Length on the SBS threshold

The dependence of the SBS threshold was investigated by carrying out SBS threshold measurements for various fibre lengths using the experimental set-up given in Figure 4-1. The results are summarized in Figure 4-12. It can be seen that the SBS threshold for both IM-DD and OFM systems reduces with increasing fibre length. However, the OFM system outperforms the IM-DD system for all fibre lengths. In other words, the OFM system delivers at least 6dB more optical power to end of the fibre link than the IM-DD system does. The launch power may exceed 60 mW for fibre lengths less than 30 km in the case of the OFM system, while for IM-DD the maximum launch power is limited to well below 37 mW (7 mW for 30 km SMF).

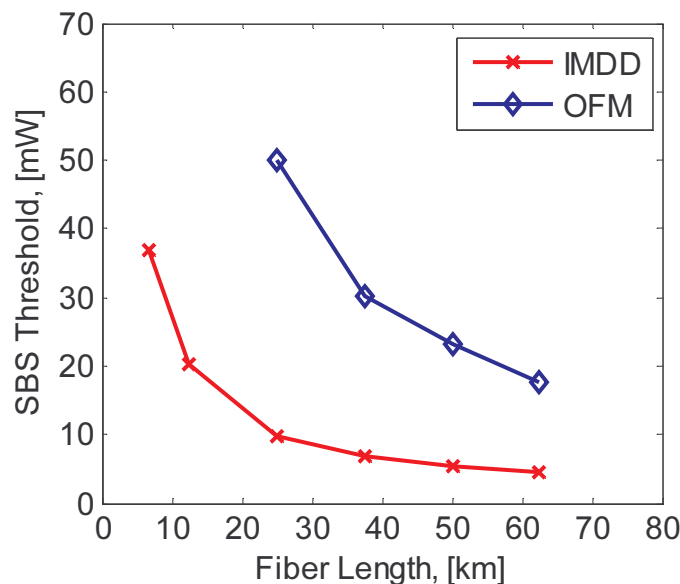


Figure 4-12 Impact of fibre length on SBS threshold

Impact of SBS on the quality of the transmitted signals

The measurement results presented in Figure 4-12 show that the OFM system performs better than the IM-DD system by allowing for more power to be transmitted over fibre links of similar lengths. However, what would be more interesting is the performance comparison between the two systems in terms of the quality of the transmitted signals. In order to investigate this, the laboratory set-up shown in Figure 4-13 was used. During the OFM system measurements the Vector Signal Generator (VSG) was used to generate a 16 QAM modulated 200 MHz sub-carrier signal. When measuring the IM-DD system performance the (modulated) signal to be transmitted was applied directly to the Intensity Modulator at the right frequency. In addition, the sweep signal and the MZI were removed during IM-DD system measurements. The power monitor/attenuator was used to maintain the detected power constant at -3 dBm.

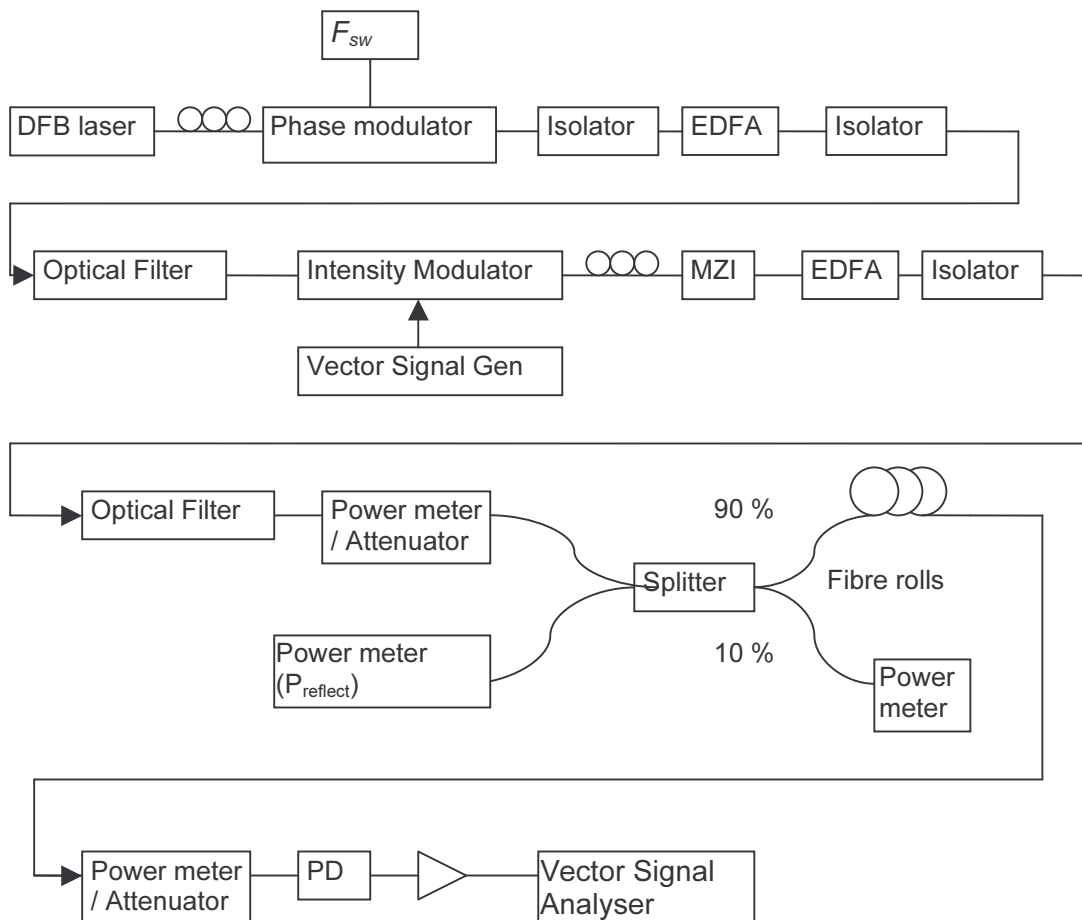


Figure 4-13 Laboratory set-up for comparing the performances of the IM-DD and the OFM RoF systems against SBS

First, the frequency of the transmitted signal in the IM-DD system was varied between 200 MHz and 18 GHz, and both the transmitted optical powers and the delivered signal quality were measured. The signal quality was measured in terms of the Error Vector Magnitude (EVM). The obtained results are given in Figure 4-14. It was observed that the quality of the transmitted signal started to deteriorate at the same time the power of the backscattered (reflected) signal began to increase sharply. This result suggests that there is a significant amount of the Stokes wave that propagates in the forward direction the moment SBS starts to take place.

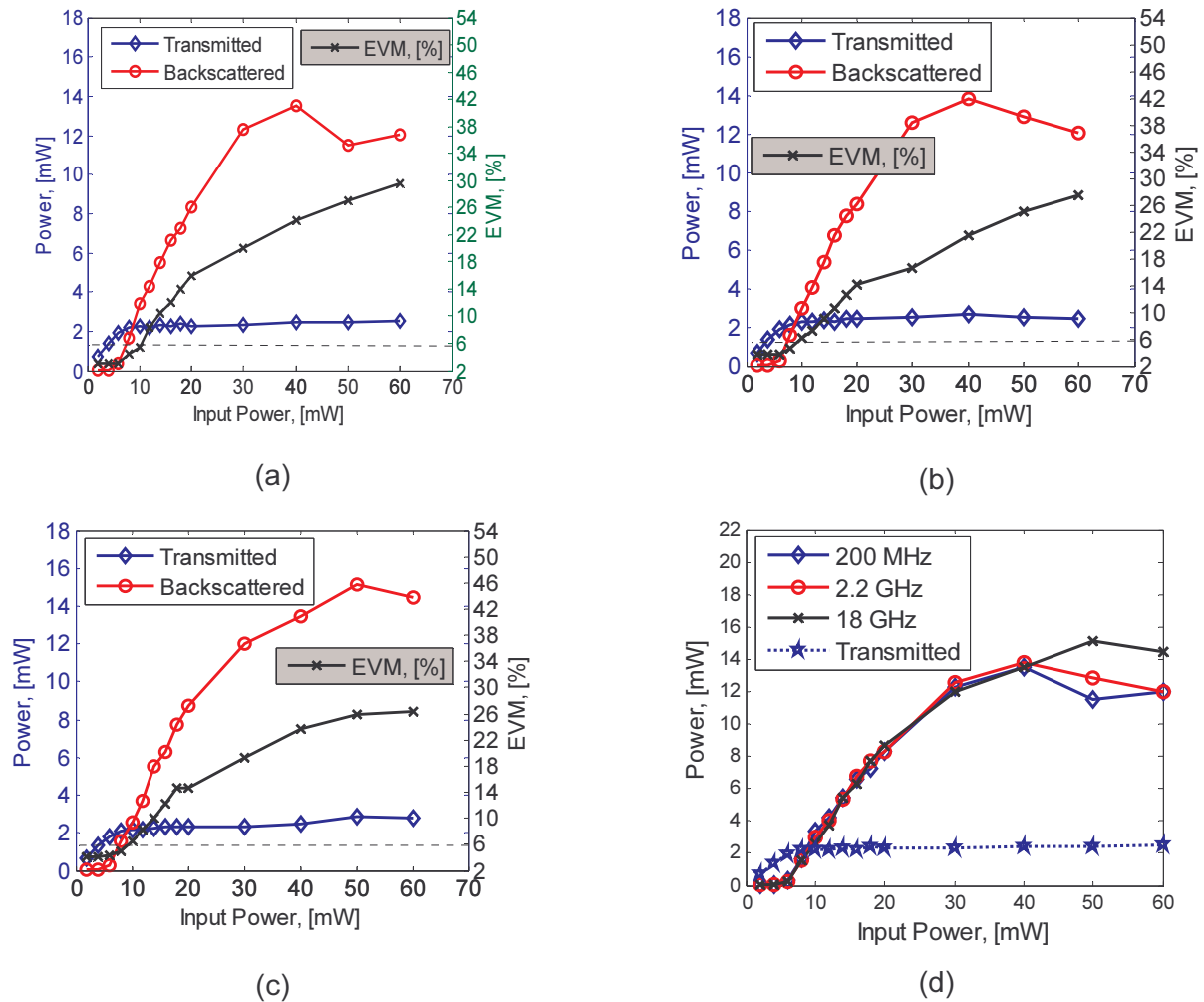


Figure 4-14 Measured impact of SBS on signal quality transmission in an IM-DD RoF system for the frequencies (a) 200 MHz, (b) 2.2 GHz, (c) 18 GHz, and (d) comparison

Figure 4-14(d) shows that the performance of the IM-DD system against SBS is independent of the frequency of the signal transmitted. This is confirmed by Figure 4-15, which shows virtually the same EVM performance for the low and high-frequency transmission. That is to say that despite the fact that transmission of higher frequencies such as 18 GHz requires much more bandwidth, this has no effect on the SBS threshold. It is concluded that what is important is the number of spectral lines in the signal, and the distribution of intensity between them, as earlier observed in the OFM system.

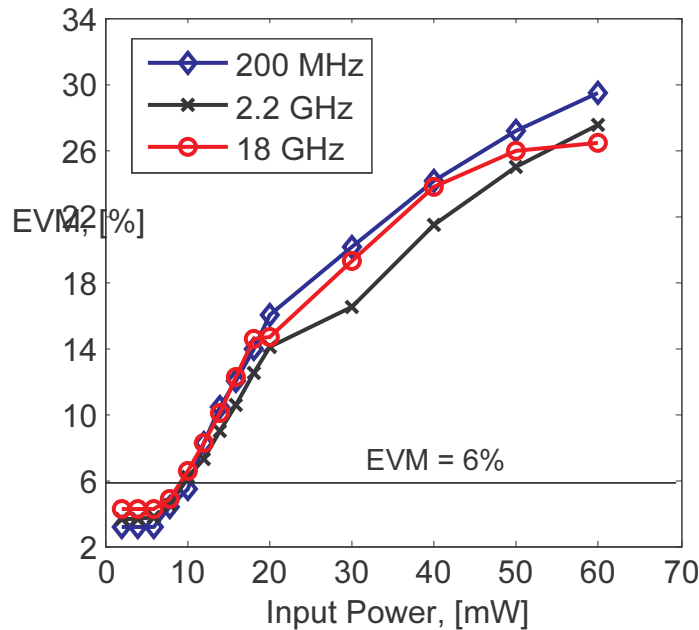


Figure 4-15 Impact of signal frequency on the performance of the IM-DD system against SBS

The performance comparison between the IM-DD and the OFM RoF systems in terms of transmitted signal quality is shown in Figure 4-16. If we assume the single carrier WiMAX standard, which defines the maximum EVM of 6% for 16 QAM modulation, then in the case of the IM-DD system, input powers are limited to less than 9 mW and 5 mW for fibre lengths of 25 km and 50 km respectively. However, in the case of the OFM system, input powers may go up to 25 mW. It is clear that the OFM system outperforms the IM-DD system for both 25 km and 50 km fibre links. In other words, the SBS effects occur at much higher input powers in the case of the OFM system. That means that longer RoF links are more feasible with OFM systems than with IM-DD systems.

Figure 4-16 shows that the performance advantage of the OFM system is greater at the longer fibre length of 50 km. In terms of the measured SNR, the OFM system outperforms the IM-DD system by more than 15 dB as shown in Figure 4-17.

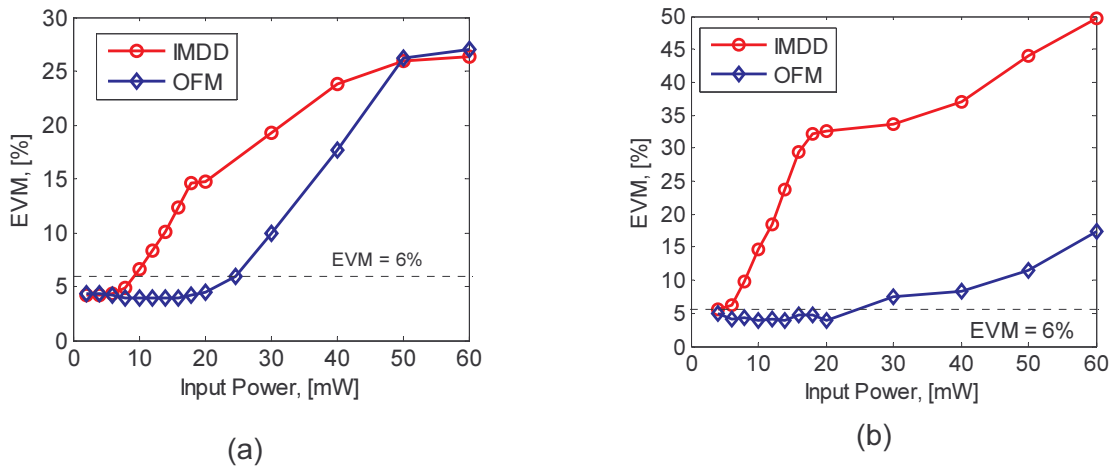


Figure 4-16 Comparison of the performances of the IM-DD (18 GHz) and the OFM (22 GHz) RoF systems against SBS (a) 25 km SMF, (b) 50 km SMF

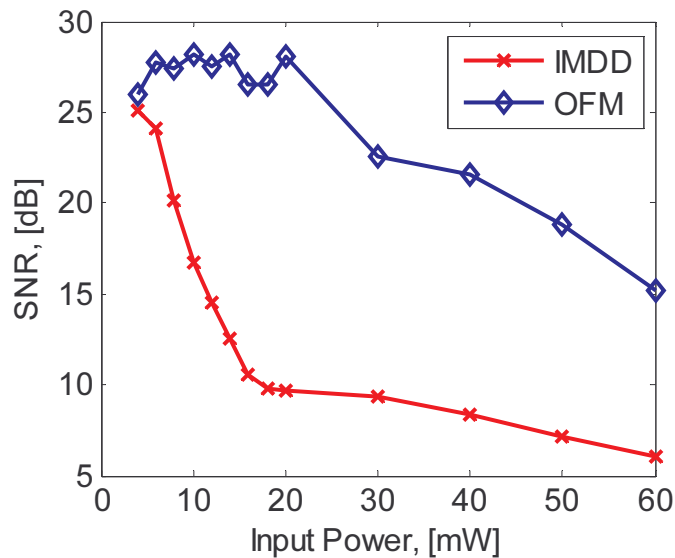


Figure 4-17 Performance comparison in terms of SNR between IM-DD and OFM RoF systems against SBS at 50 km fibre length

Measurement of the SBS gain spectrum

The SBS gain spectrum for both the IM-DD and the OFM systems was measured by using the experimental set-up given in Figure 4-18. The optical source from the DFB laser was split into two parts. One part was amplified fed through the IM-DD or OFM systems before being launched into the optical fibre via a 50% coupler. The backscattered signal was then combined with the other part of the un-modulated optical source, detected and displayed on the spectrum analyser as shown.

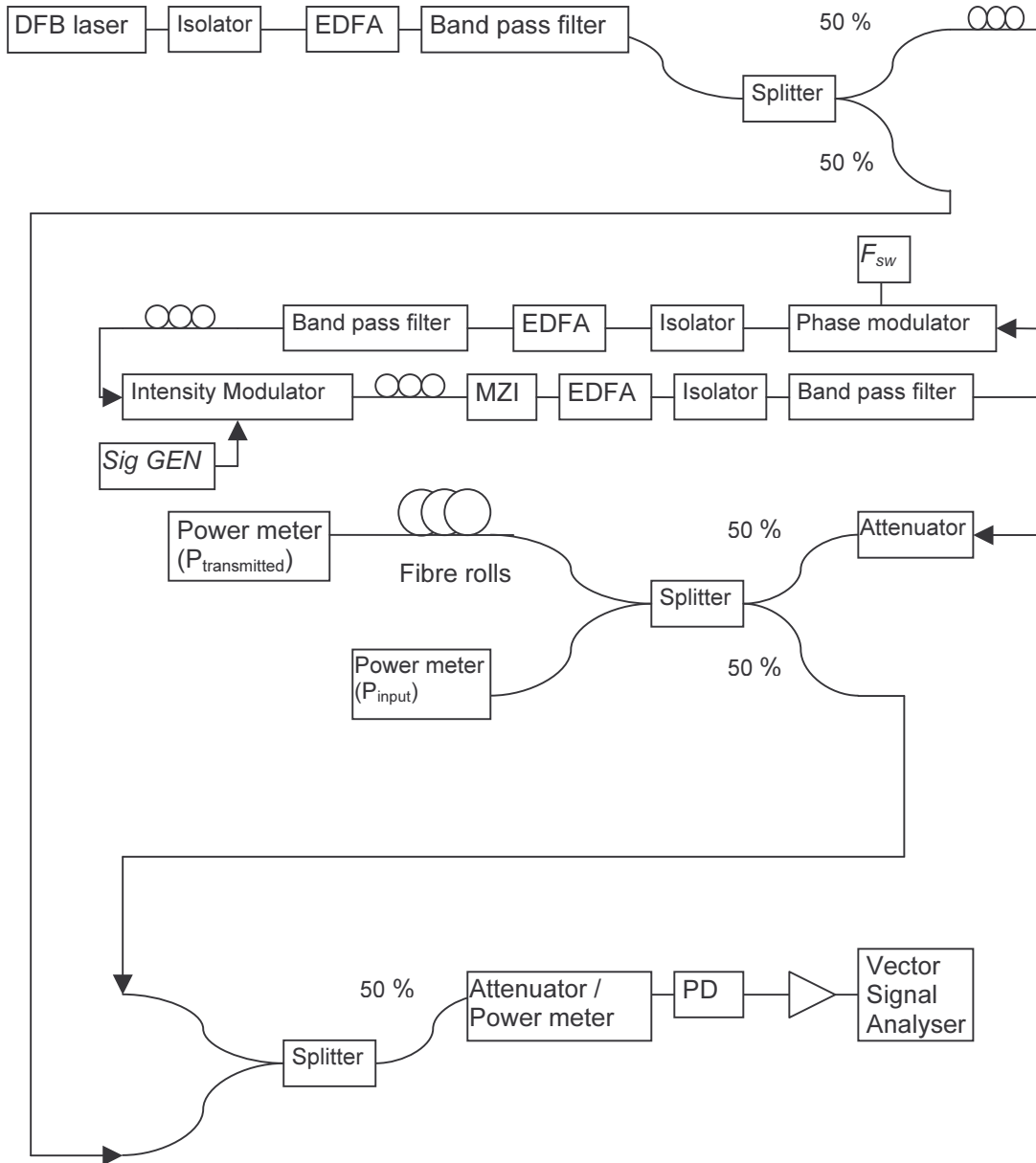


Figure 4-18 Measurement set-up used to determine the SBS gain spectrum

Gain spectrum curves were obtained for different input powers and two fibre lengths, namely 25 km and 50 km. The gain spectrum was recorded around 10.7 GHz as expected. Furthermore, it was observed for both the IM-DD and the OFM systems that for input powers below the SBS thresholds determined above, the peak values of the SBS gain coefficients were very small or non-existent as expected. However, in all measurements, the peak of OFM system was much smaller than that of the IM-DD system. For example, Figure 4-19 shows the comparison between the gain spectra of the IM-DD and the OFM systems for 25 km SMF and 20 mW input power. As shown, the peak of the IM-DD system is about 30 dBs higher. These results are consistent with the SBS threshold measurement results discussed above and with theory, since a low peak gain coefficient corresponds to a higher SBS threshold.

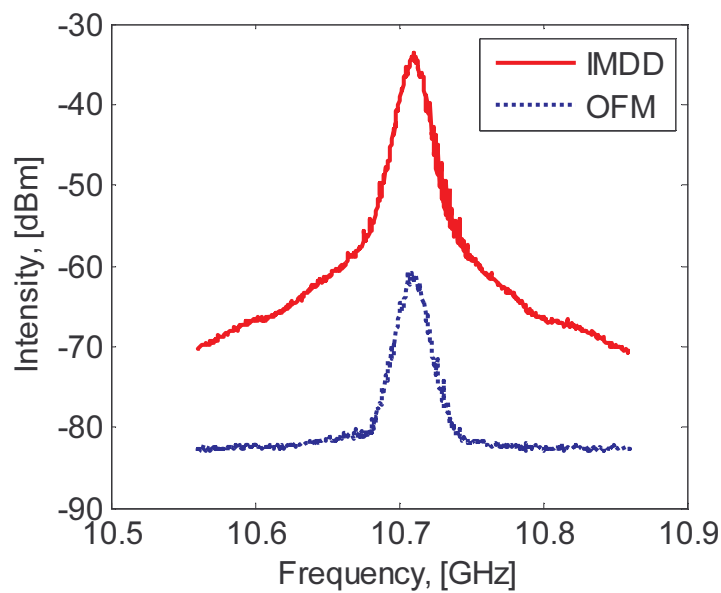


Figure 4-19 Measured SBS gain spectra for the IM-DD and the OFM RoF systems for 25 km SMF and 20 mW input power

4.2 Dispersion tolerance and model validation

In the validation with experimental values the model was tuned by finding an optimal β and by biasing the optical frequency with the MZI, the remaining parameters are given in Table 3-1.

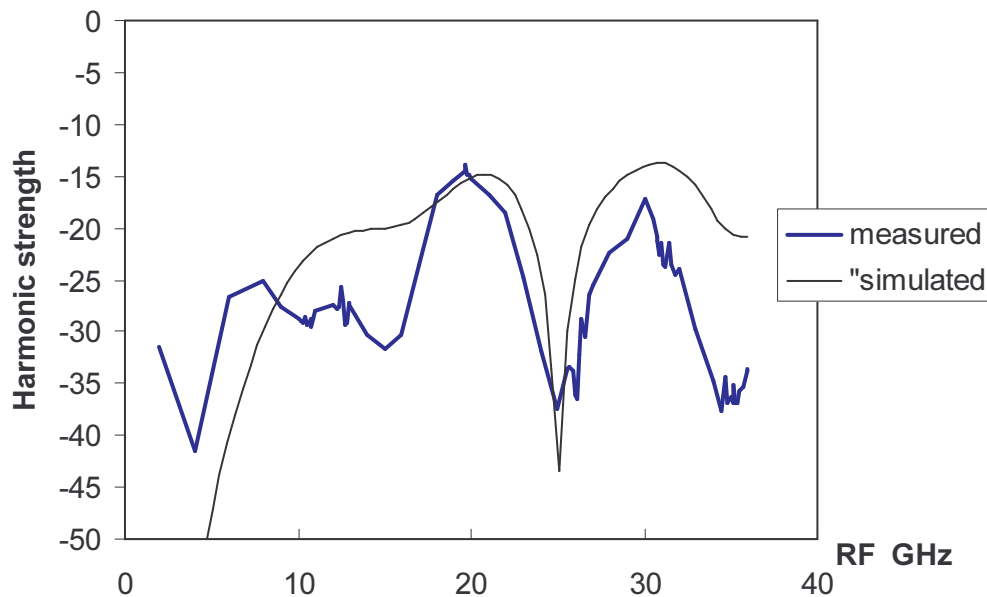


Figure 4-20 Simulations and measurements of the 5th harmonic for sweep frequencies between 0.1 and 7 GHz, at a fibre length of 25 km

OFM system measurements and model simulations for a range of sweep frequencies are depicted in Figure 4-20. The figure shows that the trend in the measurements and model predictions agree but there are discrepancies between the levels. The peak near 20 GHz is related to fibre dispersion, which followed from a closer analysis using (7). The peak at 30 GHz is due to interaction between the fibre dispersion and the interferometric filtering. At 25 GHz a large dip is present in both the measurements and the simulations. This dip is predicted by (11) since the corresponding value of the sweep frequency is equal to 5 GHz, which satisfies (10). Here the OFM-fibre system behaves like a dispersive system. The discrepancies have not been investigated further.

Figure 4-21 depicts measurements and simulations for different fibre lengths. Here the trend and the levels in the measurements and model predictions are well in agreement. The experimental values (shown as dots) illustrate that the OFM system did not suffer any fading throughout the 72 km fibre span. In addition the experiment confirmed the theoretical prediction that OFM is dispersion tolerant.

In Figure 4-21 a gain can be observed between fibre lengths 20 and 60 km in both the measurements and the simulations. In this range the FM-IM conversion is dominated by the fibre dispersion which was already mentioned in section 3.1.2. For fibre lengths outside the 20-60 km range all interaction components contribute to the overall strength. The tolerance is obviously an effect of both the fibre dispersion and the interaction between dispersion and interferometric filtering. No deep nulls occur for these parameters.

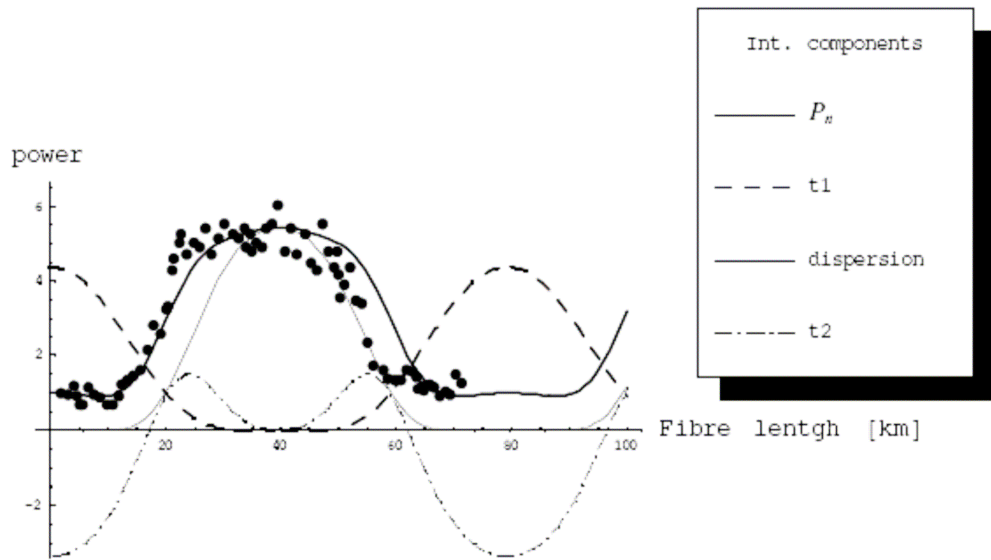


Figure 4-21 Simulations and measurements of 5th harmonic, f_m is 4.4 GHz for different fibre lengths. Measurements are displayed as dots.

5 CONCLUSIONS AND DISCUSSION

The operability of the OFM system to provide FWA services over long fibre links has been studied with experiments and theoretical work.

A theoretical model describing the behaviour of the OFM system in the presence of chromatic dispersion has been developed. The model shows that no fading occurs in the OFM distribution system. Laboratory experiments were conducted to confirm the predicted behaviour. The measurement results proved that no fading occurs in the OFM system as observed in an IM-DD system.

It is observed that both the interferometric filtering and the fibre chromatic dispersion contribute to the generation of sweep frequency harmonics. A gain occurred which can be attributed to fibre dispersion in accordance with model simulations. The model shows that OFM does not exhibit fading at certain fibre lengths as is the case with FM-IM conversion due to chromatic dispersion only. The dispersion tolerance ensues from the presence of the other interaction terms which do not vanish at these fibre lengths. However, fading can occur in the OFM system for sweep frequencies given by (10) and (12) or an integer multiple of these values for respectively odd and even harmonics. In these specific cases all components are determined by chromatic dispersion. Therefore, the associated sweep frequencies are not to be used in an operational OFM system.

The presented model and derived expressions can serve to determine optimal operation parameters for experiments with the OFM system.

Optical Frequency Multiplication can be used to combat chromatic dispersion-induced fading, enabling flexible extra-long RoF links for distributing pure high-frequency signals. In laboratory experiments, a high quality 22.2 GHz signal was transmitted over various fibre lengths up-to 72 km without any fading. The measured OFM link length was at least 15 times longer than that of the corresponding IM-DD system. The transmission of a high quality 100Mbps, 16 QAM signal at the frequency of 39.9 GHz over a 50 Km fibre length without any fading has also been demonstrated. The measured results are strongly supported by theoretical modeling and system simulations. Simulations revealed that fibre lengths up to 100 km are also feasible. The best performance of the OFM system against chromatic dispersion was found to occur when the system was optimized for maximum harmonic power generation (e.g. by appropriate filter biasing) prior to fibre transmission.

The impact of SBS on both the links lengths and the signal quality transmission of both IM-DD and OFM RoF systems was studied experimentally and compared. It was observed that the OFM system exhibited a much lower SBS threshold (6 dB) than the IM-DD system. The performance of the OFM system in terms of the quality of the transmitted signal was also found to be much better than that of the IM-DD system. Measurement results showed that longer RoF link lengths are feasible when the OFM technique is used. SBS measurement results also showed that the signal frequency has no impact on the SBS threshold and the performance of the IM-DD system.

The impact of ASE (Amplified Spontaneous Emission) noise on the RoF quality also has been evaluated. Laboratory measurements show the effects of ASE noise do not affect the transmission and the system performance in the OFM system. Only if the input signal to the EDFA is very weak, an optical filter is needed to remove the ASE noise. In the OFM system, the presence of this optical filter to remove the ASE noise is not necessary, therefore decreasing infrastructure costs.

REFERENCES

1. T. Koonen, A. Ng'oma, H. P. A. vd. Boom, I. Tafur Monroy, P. F. M. Smulders, and G. D. Khoe, "Carrying microwave signals in a GIPOF-based wireless LAN", in Proceedings of the Plastic Optical Fibres Conference, 2001, pp 217 – 223
2. Ng'Oma, A., Rijckenberg, G.-J., & Koonen, A.M.J. (2007). Building extended-reach radio-over-fibre links by exploiting optical frequency multiplication's dispersion tolerance. In proc. IEEE MTT-S International Microwave Symposium2007 . Honolulu: IEEE.
3. T. Koonen and A. Ng'oma, Chapter 11: Integrated Broadband Optical Fibre-Wireless LAN Access Networks, pp. 251-266 in: Broadband Optical Access Networks and Fiber-to-the-Home - Systems Technologies and Deployment Strategies edited by Chinlon Lin John Wiley & Sons, Ltd., England, 2006 ISBN 978-0-470-09478-5
4. Watson, G.N.: 1996, A Treatise on the Theory of Bessel Functions, Cambridge University Press, New York
5. N.G. Walker, D. Wake and I.C.Smith. "Efficient Millimetre-Wave Signal Generation Through FM-IM Conversion in Dispersive Optical Fibre Links", Electron. Lett., vol. 28, pp. 2027-2028, 1992.